EXTENDING GEOMETRIC SINGULAR PERTURBATION THEORY TO NONHYPERBOLIC POINTS—FOLD AND CANARD POINTS IN TWO DIMENSIONS*

M. KRUPA†‡ AND P. SZMOLYAN†

Abstract. The geometric approach to singular perturbation problems is based on powerful methods from dynamical systems theory. These techniques have been very successful in the case of normally hyperbolic critical manifolds. However, at points where normal hyperbolicity fails, the well-developed geometric theory does not apply. We present a method based on blow-up techniques, which leads to a rigorous geometric analysis of these problems. A detailed analysis of the extension of slow manifolds past fold points and canard points in planar systems is given. The efficient use of various charts is emphasized.

1. Introduction. We consider singularly perturbed ordinary differential equations (ODEs) in the standard form

$$(1.1) \qquad \begin{array}{rcl} \varepsilon\dot{x} & = & f(x,y,\varepsilon), \\ \dot{y} & = & g(x,y,\varepsilon), \end{array} \qquad x \in \mathbb{R}^n, \quad y \in \mathbb{R}^m, \quad 0 < \varepsilon \ll 1,$$

where f, g are C^k-functions with $k \geq 3$. Properties of solutions of (1.1) can be studied using geometric methods from dynamical systems theory. This approach, known as *geometric singular perturbation theory*, has been very successful in many contexts, yet has encountered difficulties in certain situations. In this article we show how some of the limitations of geometric singular perturbation theory can be removed.

Before describing our results we present a brief survey of the existing theory. Let τ denote the independent variable in (1.1). The variable τ is referred to as the *slow* time scale. By switching to the *fast* time scale $t := \tau/\varepsilon$ one obtains the equivalent system

$$(1.2) \qquad \begin{array}{rcl} x' & = & f(x,y,\varepsilon), \\ y' & = & \varepsilon g(x,y,\varepsilon). \end{array}$$

One tries to analyze the dynamics of (1.1) by suitably combining the dynamics of the *reduced problem*

$$(1.3) \qquad \begin{array}{rcl} 0 & = & f(x,y,0), \\ \dot{y} & = & g(x,y,0) \end{array}$$

---

†Institut für Angewandte und Numerische Mathematik, Technische Universität Wien, Wiedner Hauptstraße 6-10, A-1040 Wien, Austria (peter.szmolyan@tuwien.ac.at). This research was supported by the Austrian Science Foundation under grant Y 42-MAT.

‡Current address: Department of Mathematical Sciences, New Mexico State University, Las Cruces, NM 88003-8001 (mkrupa@nmsu.edu).

and the dynamics of the *layer problem*

$$(1.4) \qquad \begin{aligned} x' &= f(x,y,0), \\ y' &= 0, \end{aligned}$$

which are the limiting problems for $\varepsilon = 0$ on the slow and the fast time scales, respectively.

The foundation of geometric singular perturbation theory was laid by Fenichel [8]. The basic reasoning is as follows. The reduced problem (1.3) is a dynamical system on the set $S := \{(x,y) \in \mathbb{R}^{n+m} : f(x,y,0) = 0\}$. In the following we refer to S as the *critical manifold*. A normally hyperbolic invariant manifold of equilibria $S_0 \subset S$ of the layer problem (1.4) persists as a locally invariant slow manifold S_ε of (1.1) for ε sufficiently small. The restriction of (1.1) to S_ε is a small smooth perturbation of the reduced problem (1.3). Moreover, there exist a stable and an unstable invariant foliation with base S_ε with the dynamics along each foliation being a small perturbation of the suitable restriction of the dynamics of (1.4). For an excellent introduction to geometric singular perturbation theory and an overview of applications, we refer the reader to the survey by Jones [11].

However, despite many efforts, points on the critical manifold S where normal hyperbolicity breaks down remained a major obstacle to the geometric theory. This was a definite shortcoming in view of the abundance of nonhyperbolic points in applications.

One cause for the breakdown of normal hyperbolicity of a critical manifold S are bifurcation points due to a zero eigenvalue of the Jacobian $\frac{\partial f}{\partial x}$. The most common case are folded critical manifolds. A well-known phenomenon in this context are relaxation oscillations, i.e., solutions slowly moving towards a fold point, jumping from the fold point to another stable branch of S, following the slow dynamics again until another fold point is reached, jumping again, etc., thus, possibly forming periodic solutions [9], [18], and [20].

Another delicate phenomenon occuring at folds are *canard solutions* which were discovered and first analyzed by Benoit, Callot, Diener, and Diener [3]; see also [2]. A canard solution is a solution of a singularly perturbed system which is contained in the intersection of an attracting slow manifold and a repelling slow manifold. The existence of a canard solution can lead to *canard explosion*, i.e., a transition from a small limit cycle to a relaxation oscillation through a sequence of *canard cycles* [3], [6], [7]. For planar vector fields canards are nongeneric and occur persistently in one-parameter families; yet in dimensions larger than two they can occur in generic situations [2], [19], [23].

In this article we show how geometric singular perturbation theory can be extended to *fold points* and *canard points* in planar systems, i.e., we restrict our attention to the case $n = m = 1$. A fold point corresponds to the situation when the critical manifold has a generic fold. Depending on the stability properties of the critical manifold and on the direction of the reduced flow, a number of cases are possible. We analyze the so-called *jump point*, for which the reduced flow is directed towards the fold. This is the situation which is relevant for relaxation oscillations. We show how the slow manifolds (existing by the normally hyperbolic theory) extend in the neighborhood of the singularity. The treatment of the fold point is a refinement of the analysis in our earlier work [13]. A canard point is a fold point with an additional degeneracy leading to a possibility of a canard solution. Again we analyze how slow manifolds extend and show that a canard solution occurs along a codimension one

curve in the parameter plane. In a complementary work [15] we carry out a similar analysis for singularities of pitchfork and transcritical type.

Our approach relies on the blow-up method, which is a way of partially desingularizing the vector field in the neighborhood of a singular point. After a blow-up transformation, standard methods from dynamical systems theory can be applied. Our proof of the existence of a canard solution is based on a variant of the Melnikov method. The blow-up method was first applied to a singular perturbation problem in the pioneering work of Dumortier and Roussarie [6], who analyzed the existence of *canard cycles* in the van der Pol equation. One of the purposes of this work is to build a bridge between the methods of [6] and geometric singular perturbation theory; in particular, we use the blow-up method to answer the question of extending slow manifolds near nonhyperbolic singularities.

The sequel of this article [14] is devoted to relaxation oscillations and canard explosion. The methods and results of this paper are of central importance in our analysis of these phenomena. Since the analysis of canard cycles is a more delicate problem, we find it advantageous to treat these issues separately. In particular, we prefer to use blow-up to obtain local results which in a second step can be used to study global phenomena. We feel that this point of view is also useful in the analysis of related problems. In this sense, our work is intended as a complement to the more global approach in the work of Dumortier [5] and Dumortier and Roussarie [6].

In this article and in [14] we restrict our attention to the planar case. However, the analysis carries over to higher-dimensional problems with one-dimensional critical manifolds containing fold points. By means of a center-manifold reduction, all normally hyperbolic directions can be eliminated and one recovers the planar problems considered here. A well-known problem where this is relevant is the traveling wave problem for the FitzHugh–Nagumo equation [11]. For a similar approach to problems with higher-dimensional critical manifolds, we refer the reader to [17] and [23].

The article is organized as follows. Section 2 contains the description and the analysis of a generic fold. Here we give a detailed expository presentation of the blow-up method. In section 3 we analyze a canard point.

2. Generic fold.

2.1. Assumptions and results. Consider the singularly perturbed ODE (1.2), where $(x, y) \in \mathbb{R}^2$ and ε is a small real parameter. Suppose that (x_0, y_0) is such that

$$(2.1) \qquad f(x_0, y_0, 0) = 0, \qquad \frac{\partial f}{\partial x}(x_0, y_0, 0) = 0.$$

Our goal is to obtain a characterization of the dynamics in a neighborhood of (x_0, y_0) for sufficiently small values of ε. We make the following nondegeneracy assumptions:

$$(2.2) \qquad \frac{\partial^2 f}{\partial x^2}(x_0, y_0, 0) \neq 0, \quad \frac{\partial f}{\partial y}(x_0, y_0, 0) \neq 0, \quad g(x_0, y_0, 0) \neq 0.$$

We assume, without loss of generality, that

$$(x_0, y_0) = (0, 0), \quad \frac{\partial^2 f}{\partial x^2}(0, 0, 0) > 0, \quad \frac{\partial f}{\partial y}(x_0, y_0, 0) < 0$$

hold.

As before let $S = \{(x, y) : f(x, y, 0) = 0\}$ be the critical manifold. The nondegeneracy assumptions imply that there exists a neighborhood U of the origin such that
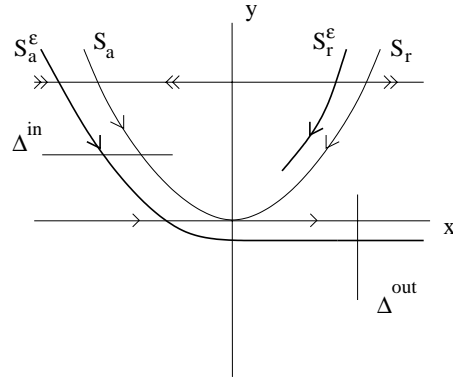
FIG. 2.1. *Critical manifold, slow manifolds, and sections for the fold point.*

$(0, 0)$ is the only point in $U \cap S$, where $\frac{\partial f}{\partial x}$ vanishes and that $S \cap U$ is approximately a parabola. Let S_a (resp., S_r) denote its left (resp., right) branch, so that $S = S_a \cup S_r$ (see Figure 2.1). The assumption $\frac{\partial^2 f}{\partial x^2}(0, 0, 0) > 0$ implies that for $y > 0$ the branch S_a is attracting and the branch S_r is repelling for the layer problem, which also explains the notation. The origin is nonhyperbolic, weakly attracting from the left and weakly repelling to the right (see Figure 2.1).

To determine the reduced dynamics we solve the equation $f(x, y, 0) = 0$ for y as a function of x, i.e., $y = \varphi(x)$. The reduced dynamics is then determined by

$$(2.3) \qquad \varphi'(x)\dot{x} = g(x, \varphi(x), 0),$$

which is singular at $x = 0$. Our assumptions on f and g imply that the direction of the reduced flow is determined by the sign of $g(0, 0, 0)$. We assume $g(0, 0, 0) < 0$. This implies that the reduced flow on S_a and S_r is directed towards the fold point; see Figure 2.1. Actually, orbits on S_a and S_r reach the fold point in finite time due to the singularity at the fold point. The only possibility to continue from there in the singular limit is along the (weakly) unstable fiber of the layer problem along the positive x-axis. Thus, the curve $S_a \cup \{(x, 0), x > 0\}$ is expected to be a zeroth order approximation. This is the situation relevant to relaxation oscillations; we refer to this case as *jump point*. The case $g(0, 0, 0) > 0$ can be analyzed similarly.

It follows from the standard theory [8] that outside an arbitrarily small neighborhood V of $(0, 0)$, the manifolds S_a and S_r perturb smoothly to locally invariant manifolds $S_{a,\varepsilon}$ and $S_{r,\varepsilon}$ for sufficiently small $\varepsilon \neq 0$. We would like to point out that $S_{a,\varepsilon}$ and $S_{r,\varepsilon}$ are actually very simple. They consist of single solutions. Note that the slow manifolds are obtained as sections $\varepsilon = $ const. of two-dimensional, locally invariant, center-like manifolds M_a (resp., M_r) of the extended system

$$(2.4) \qquad \begin{aligned} x' &= f(x, y, \varepsilon), \\ y' &= \varepsilon g(x, y, \varepsilon), \\ \varepsilon' &= 0 \end{aligned}$$

in the extended phase space $\mathbb{R}^3$. For this extended system $S \times \{0\}$ is a manifold of equilibria. Outside of a neighborhood of the fold point $(0, 0, 0)$ the linearization of system (2.4) at points $S_a \times \{0\}$ has a double zero eigenvalue and one uniformly hyperbolic (stable) eigenvalue. This allows us to conclude the existence of the attracting

center-like manifold M_a; the manifold M_r is obtained in a similar way. At the fold point $(0, 0, 0)$ the linearization has a triple eigenvalue zero and the construction of the slow manifolds breaks down. We focus our attention on S_a and investigate how $S_{a,\varepsilon}$ as well as nearby solutions behave as they pass near the fold point. We expect that close to the fold point a transition from slow motion along $S_{a,\varepsilon}$ to a fast motion almost parallel to the unstable fibers occurs. A similar analysis could be carried out for $S_{r,\varepsilon}$.

Remark 2.1. It is known that the slow manifolds M_a and M_r and hence their sections $S_{a,\varepsilon}$ and $S_{r,\varepsilon}$ are not unique and are determined only up to $O(e^{-c/\varepsilon})$, where c is some positive constant. We make an arbitrary choice of M_a and M_r and indicate at the end that our results are independent of this choice.

We now view the previously introduced neighborhood U as a neighborhood of $(0, 0, 0)$ in $\mathbb{R}^3$. We pick U sufficiently small, so that $g(x, y, \varepsilon) \neq 0$ for $(x, y, \varepsilon) \in U$. Before stating the main results we rewrite system (1.2) (resp., (2.4)) in a canonical form. By rescaling x, y, ε, and t we obtain

$$
\begin{aligned}
x' &= -y + x^2 + h(x, y, \varepsilon), \\
y' &= \varepsilon g(x, y, \varepsilon), \\
\varepsilon' &= 0
\end{aligned}
\tag{2.5}
$$

with $h(x, y, \varepsilon) = O(\varepsilon, xy, y^2, x^3)$, $g(x, y, \varepsilon) = -1 + O(x, y, \varepsilon)$, where the new function g is related to the original one by the rescaling. This form of the equations will be used throughout the forthcoming analysis.

For small $\rho > 0$ and a suitable interval $J \subset \mathbb{R}$ let

$$
\Delta^{in} = \{(x, \rho^2), x \in J\}
$$

be a section in U transverse to S_a and let

$$
\Delta^{out} = \{(\rho, y), y \in \mathbb{R}\}
$$

be a section in U transverse to the fast fibers (see Figure 2.1). Note, that the same constant ρ is used throughout this paper.

Let $\pi : \Delta^{in} \to \Delta^{out}$ be the transition map for the flow of (1.2).

THEOREM 2.1. *Under the assumptions made in this section there exists $\varepsilon_0 > 0$ such that the following assertions hold for $\varepsilon \in (0, \varepsilon_0]$:*
1. *The manifold $S_{a,\varepsilon}$ passes through Δ^{out} at a point $(\rho, h(\varepsilon))$, where $h(\varepsilon) = O(\varepsilon^{2/3})$.*
2. *The transition map π is a contraction with contraction rate $O(e^{-c/\varepsilon})$, where c is a positive constant.*

In the context of matched asymptotic expansions assertion (1) of the theorem is well known; see, e.g., [18]. A blow-up based derivation of the asymptotic expansion of $h(\varepsilon)$ is given in [16]. Assertion (2) of the theorem explains why the nonuniqueness of the slow manifold M_a (resp., $S_{a,\varepsilon}$) does not affect our results. Two different choices of these manifolds are exponentially close at Δ^{in} and even more so at Δ^{out} due to the exponential contraction during the passage.

2.2. Blow-up. In this section we define and describe the blow-up transformation. The basic observation is that the fold point $(0, 0, 0)$ is a more degenerate equilibrium point of system (2.5) than the other points of the critical manifold S. The

linearization of system (2.5) at the origin has a triple zero eigenvalue while the linearization at the other points of the critical manifold S has a double zero eigenvalue and one negative (resp., positive) eigenvalue for $x < 0$ (resp., $x > 0$).

The important insight in [6] is that blow-up techniques are the right tool to analyze nilpotent equilibria like the fold point, viewed as a degenerate equilibrium of the extended system (2.4). The blow-up method is essentially a clever coordinate transformation by which the degenerate equilibrium is "blown-up" to a two-sphere. In certain directions transverse to the sphere and even on the sphere, one gains enough hyperbolicity to allow a complete analysis by standard techniques. The technique is a generalization of the well known blow-up methods for degenerate equilibria of planar vector fields [5]. In the simplest situations this corresponds to blowing-up the degenerate equilibrium to the circle $r = 0$ by rewriting the vector field in polar coordinates $(r, \vartheta) \in \mathbb{R} \times S^1$. The analysis is often simplified substantially by using a quasi-homogeneous blow-up, i.e. by using different powers (weights) of r for different variables in the defining transformation.

The blow-up transformation for system (2.5) is

$$(2.6) \qquad x = \bar{r}\bar{x}, \quad y = \bar{r}^2\bar{y}, \quad \varepsilon = \bar{r}^3\bar{\varepsilon}$$

with weights 1, 2, and 3. We define $B = S^2 \times [0, \rho]$, where the constant $\rho > 0$ is related to ε_0 by $\varepsilon_0 = \rho^3$. We consider the blow-up transformation as a mapping

$$(2.7) \qquad \Phi : B \to \mathbb{R}^3$$

with $(\bar{x}, \bar{y}, \bar{\varepsilon}) \in S^2$. We choose $\rho > 0$ sufficiently small such that system (2.4) is described by the canonical form (2.5) in the region $\Phi(B)$. We will be interested only in nonnegative values of $\bar{\varepsilon}$ and $\bar{r}$, but everything that follows makes sense for negative values as well, i.e., there are no technical problems at ∂B.

Let X denote the vector field corresponding to (2.5). Since X vanishes at the point $(0, 0, 0)$, there exists a vector field $\bar{X}$ on B such that $\Phi_* \bar{X} = X$, where Φ_* is induced by Φ. It remains to study the vector field $\bar{X}$ on the manifold B. Note that this suffices, since $\Phi(B)$ is a full neighborhood of the origin. In principle one could use spherical coordinates on S^2; however, this would lead to rather lengthy computations. It is natural and almost mandatory to use different charts for the manifold B to simplify the analysis. One reason for this is that—as we will see later—the dynamics in the individual charts is very different.

We will now introduce the charts used later in this paper. Loosely speaking, we will define a chart K_2, which describes a neighborhood of the upper half-sphere defined by $\bar{\varepsilon} > 0$, and charts K_1 and K_3 which describe neighborhoods of parts of the equator of S^2 which are needed in the analysis. In problems where a neighborhood of the whole equator needs to be analyzed, two further charts must be defined analogously. The subscripts in K_1, K_2, and K_3 denote the order in which the charts are used later.

The charts K_1, K_2, and K_3 are obtained by setting $\bar{y} = 1$, $\bar{\varepsilon} = 1$, and $\bar{x} = 1$, respectively, in the blow-up transformation (2.6). The blow-up transformation in the charts K_i, $i = 1, 2, 3$ is given by

$$(2.8) \qquad x = r_1 x_1, \quad y = r_1^2, \quad \varepsilon = r_1^3 \varepsilon_1,$$

$$(2.9) \qquad x = r_2 x_2, \quad y = r_2^2 y_2, \quad \varepsilon = r_2^3,$$

$$(2.10) \qquad x = r_3, \quad y = r_3^2 y_3, \quad \varepsilon = r_3^3 \varepsilon_3$$

with coordinates $(x_1, r_1, \varepsilon_1) \in \mathbb{R}^3$, $(x_2, y_2, r_2) \in \mathbb{R}^3$, and $(r_3, y_3, \varepsilon_3) \in \mathbb{R}^3$. The point $(0,0,0)$ is blown-up to the plane $r_i = 0$, $i = 1, 2, 3$. In our analysis we will need to change coordinates between these charts on their overlap domains. A simple computation gives the following lemma.

LEMMA 2.2. *Let κ_{12} denote the change of coordinates from K_1 to K_2. Then κ_{12} is given by*

$$(2.11) \qquad x_2 = x_1 \varepsilon_1^{-1/3}, \quad y_2 = \varepsilon_1^{-2/3}, \quad r_2 = r_1 \varepsilon_1^{1/3} \quad \text{for } \varepsilon_1 > 0,$$

and κ_{12}^{-1} is given by

$$(2.12) \qquad x_1 = x_2 y_2^{-1/2}, \quad r_1 = r_2 y_2^{1/2}, \quad \varepsilon_1 = y_2^{-3/2} \quad \text{for } y_2 > 0 .$$

Let κ_{23} denote the change of coordinates from K_2 to K_3. Then κ_{23} is given by

$$(2.13) \qquad r_3 = r_2 x_2, \quad y_3 = y_2 x_2^{-2}, \quad \varepsilon_3 = x_2^{-3} \quad \text{for } x_2 > 0,$$

and κ_{23}^{-1} is given by

$$(2.14) \qquad x_2 = \varepsilon_3^{-1/3}, \quad y_2 = y_3 \varepsilon_3^{-2/3}, \quad r_2 = r_3 \varepsilon_3^{1/3} \quad \text{for } \varepsilon_3 > 0 .$$

The above constructions make perfect sense if restricted to B. We introduce the following notation: $\bar{P}$ denotes an object in the blow-up which corresponds to an object P in the original problem. If $\bar{P}$ is described in one of the charts, then P_i denotes the object in chart K_i, $i = 1, 2, 3$. This notation is used only when necessary, mostly to denote various invariant manifolds.

Remark 2.2. In the work of Dumortier and Roussarie the chart K_2 corresponding to a directional blow-up in the direction of ε is called *family rescaling*, and charts used near the equator are called *phase directional rescaling*.

2.3. Blow-up of (1.2) with $\varepsilon = 0$. It is instructive to recall how the usual blow-up method applies to the layer problem, i.e., system (2.5) with $\varepsilon = 0$. Setting $\bar{\varepsilon} = 0$ in (2.6) defines a (planar, polar) blow-up of the degenerate equilibrium at the origin. To see this, note that $B \cap \{\bar{\varepsilon} = 0\} = S^1 \times [0, \rho]$, where $S^1 = \{(\bar{x}, \bar{y}, 0) \in S^2\}$. Due to the equation $\varepsilon' = 0$, the set $S^1 \times [0, \rho]$ is invariant for $\bar{X}$, which, restricted to $S^1 \times [0, \rho]$, is the blow-up of (1.2) with $\varepsilon = 0$.

Let $\bar{X}_0 = \bar{X}|_{S^1 \times [0,\rho]}$. Figure 2.2 shows the phase portrait of $\bar{X}_0$. We briefly describe this phase portrait, referring the reader to the sections on charts K_1 and K_3 for technical details. On the invariant circle S^1, there are four equilibria: p_a, p_r, q_{in}, q_{out}. These equilibria are hyperbolic for the flow on S^1, the points p_a and q_{out} are attracting, and p_r and q_{in} are repelling. The points p_a and p_r are end points of the blown-up critical manifolds $\bar{S}_a$ and $\bar{S}_r$, which are lines of equilibria for $\bar{X}_0$. Hence the radial direction is nonhyperbolic at p_a and p_r. The points q_{in} and q_{out} are the intersection points of S^1 with the blow-up of the critical fiber. These points are hyperbolic in the radial direction.

2.4. Dynamics in chart K_2. The dynamics of the blown-up vector field $\bar{X}$ in a neighborhood of the upper half-sphere is studied in chart K_2. The transformation (2.9) is just a rescaling of (x, y), since $r_2 = \varepsilon^{1/3}$. By inserting (2.9) into system (2.5) we obtain the vector field $\bar{X}$ in chart K_2. Since $r_2' = 0$, this blown-up system is still a
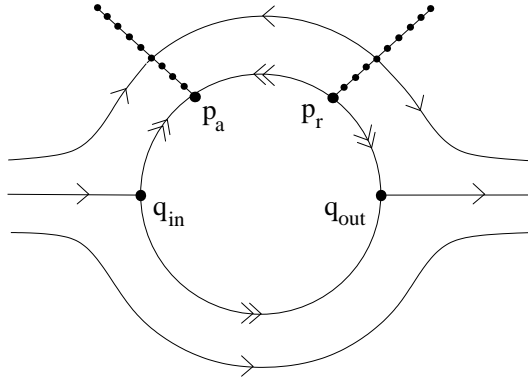
FIG. 2.2. *Phase portrait of the blown-up vector field for $\bar{\varepsilon} = 0$.*

family of planar vector fields with parameter r_2. We now desingularize the equations by rescaling time $t_2 := r_2 t$, so that the factor r_2 disappears. This desingularization is necessary to obtain a nontrivial flow on the blown-up locus $r_2 = 0$. We obtain

$$(2.15) \qquad \begin{aligned} x_2' &= x_2^2 - y_2 + O(r_2), \\ y_2' &= -1 + O(r_2), \\ r_2' &= 0, \end{aligned}$$

where $'$ denotes differentiation with respect to t_2.

Remark 2.3. The rescaled form (2.15) of the original problem plays a crucial role in all approaches to the fold point by means of asymptotic expansions; e.g. [12], [18], and [20]. In these investigations solutions of (2.15) are used as inner solutions connecting (*matching*) solutions obtained as perturbations of the reduced problem to solutions obtained as solutions of the layer problem.

We first consider the case $r_2 = 0$, which gives

$$(2.16) \qquad \begin{aligned} x_2' &= x_2^2 - y_2, \\ y_2' &= -1. \end{aligned}$$

This is a Riccati equation whose solutions can be expressed in terms of special functions. The relevant results can be found in [18, pp. 68–72]. Here we restate the results needed in our analysis. For the sake of readability we omit the subscript 2 of the variables.

PROPOSITION 2.3 (see [18]). *The Riccati equation* (2.16) *has the following properties:*

1. *Every orbit has a horizontal asymptote $y = y_r$, where y_r depends on the orbit such that $x \to \infty$ as y approaches y_r from above.*
2. *There exists a unique orbit γ_2 which can be parametrized as $(x, s(x))$, $x \in \mathbb{R}$ and is asymptotic to the left branch of the parabola $x^2 - y = 0$ for $x \to -\infty$. The orbit γ_2 has a horizontal asymptote $y = -\Omega_0 < 0$ such that $x \to \infty$ as y approaches $-\Omega_0$ from above.*
3. *The function $s(x)$ has the asymptotic expansions*

$$s(x) = x^2 + \frac{1}{2x} + O\left(\frac{1}{x^4}\right), \quad x \to -\infty,$$

$$s(x) = -\Omega_0 + \frac{1}{x} + O\left(\frac{1}{x^3}\right), \quad x \to \infty.$$

4. *All orbits to the right of γ_2 are backward asymptotic to the right branch of the parabola $x^2 - y = 0$.*

5. *All orbits to the left of γ_2 have a horizontal asymptote $y = y_l > y_r$, where y_l depends on the orbit, such that $x \to -\infty$ as y approaches y_l from below.*

Remark 2.4. The constant Ω_0 is the smallest positive zero of

$$J_{-1/3}(2z^{3/2}/3) + J_{1/3}(2z^{3/2}/3),$$

where $J_{-1/3}$ (resp., $J_{1/3}$) are Bessel functions of the first kind [18].
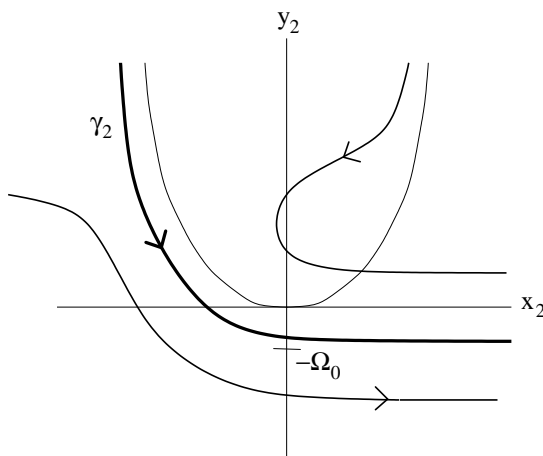

FIG. 2.3. *Solutions of the Riccati equation* (2.16).

The assertions of Proposition 2.3 are illustrated in Figure 2.3. We will see that the orbit $\bar{\gamma}$ corresponding to the special solution γ_2 is backward asymptotic to the equilibrium p_a on the equator of S^2. The importance of the orbit $\bar{\gamma}$ is that it "leads" the incoming attracting slow manifold across the upper half of the sphere S^2 to the point q_{out} from where take-off in the direction of the fast flow occurs.

We need to describe the transition map for (2.15) within a bounded domain D_2. Within such a domain we can deduce properties of the flow of (2.15) from Proposition 2.3 by using regular perturbation theory. A detailed study of the effect of the $O(r_2)$ perturbations outside D_2, i.e., close to infinity, will be carried out in the charts K_1 and K_3. For $\delta > 0$ we define the following sections:

$$\Sigma_2^{in} = \{(x_2, y_2, r_2) : y_2 = \delta^{-2/3}\}, \quad \Sigma_2^{out} = \{(x_2, y_2, r_2) : x_2 = \delta^{-1/3}\}.$$

Let Π_2 be the transition map of the flow (2.15) from Σ_2^{in} to Σ_2^{out}. Let $q_0 = \gamma_2 \cap \Sigma_2^{in}$.
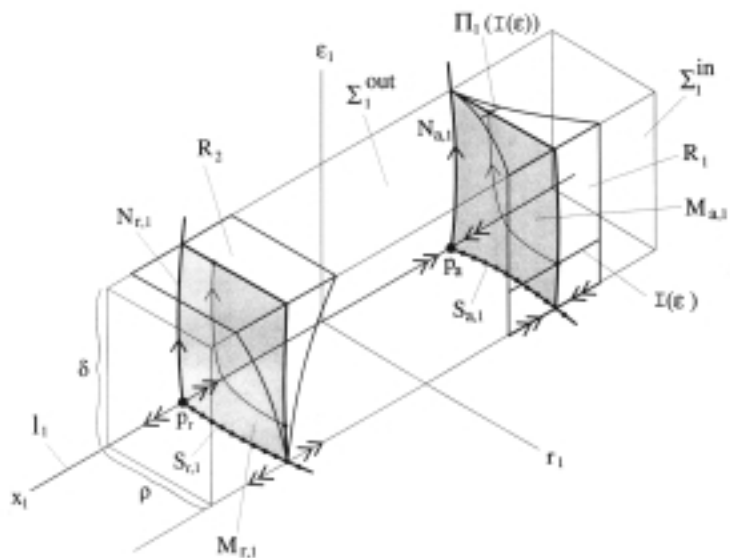
PROPOSITION 2.4. *The transition map Π_2 has the following properties:*

1.

$$\Pi_2(q_0) = (\delta^{-1/3}, -\Omega_0 + \delta^{1/3} + O(\delta), 0).$$

2. *A neighborhood of q_0 is mapped diffeomorphically onto a neighborhood of $\Pi_2(q_0)$.*

Proof. The proof follows directly from Proposition 2.3 and regular perturbation theory. □

FIG. 2.4. *Geometry and dynamics in chart K_1.*

2.5. Dynamics in chart K_1. Chart K_1 is used to analyze the dynamics of the blown-up vector field $\bar{X}$ in a neighborhood of the equator containing the equilibria p_a and p_r. By inserting (2.8) into system (2.5), we obtain the vector field $\bar{X}$ in chart K_1. We desingularize the blown-up vector field $\bar{X}$ by dividing by r_1. This gives

$$x_1' = -1 + x_1^2 + \frac{1}{2}\varepsilon_1 x_1 + O(r_1),$$

(2.17) $$r_1' = \frac{1}{2}r_1\varepsilon_1(-1 + O(r_1)),$$

$$\varepsilon_1' = \frac{3}{2}\varepsilon_1^2(1 + O(r_1)),$$

where $'$ denotes differentiation with respect to a rescaled time variable t_1.

Remark 2.5. The equation for ε_1' is obtained from the equation $\varepsilon' = 0$, which implies the relation $3r_1^2 r_1' \varepsilon_1 + r_1^3 \varepsilon_1' = 0$. Hence $\varepsilon = r_1^3 \varepsilon_1$ is a constant of motion in chart K_1. Nevertheless, we will see that it is useful to treat the blown-up system as a three-dimensional problem. This seemingly artificial construction is actually crucial for the whole approach.

Remark 2.6. For $r_1 > 0$, system (2.17) has the same orbits as the blown-up vector field $\bar{X}$ with the corresponding solutions having a different time parametrization. Since we deal only with transition maps between sections, time parametrization of solutions has no significance to our analysis.

System (2.17) has two invariant subspaces, namely, the plane $r_1 = 0$ and the plane $\varepsilon_1 = 0$. Their intersection is the invariant line $l_1 := \{(x_1, 0, 0) : x_1 \in \mathbb{R}\}$; see Figure 2.4. The dynamics on l_1 is governed by $x_1' = -1 + x_1^2$. There are two

equilibria $p_a = (-1, 0, 0)$ and $p_r = (1, 0, 0)$. For the flow on the line l_1 both points are hyperbolic, the relevant eigenvalue is -2 for p_a and 2 for p_r, i.e., p_a is attracting and p_r is repelling. The dynamics in the invariant plane $\varepsilon_1 = 0$ is governed by

$$(2.18) \qquad \begin{aligned} x_1' &= -1 + x_1^2 + O(r_1), \\ r_1' &= 0. \end{aligned}$$

This system has a normally hyperbolic curve $S_{a,1}$ of equilibria emanating from p_a and a curve $S_{r,1}$ of equilibria emanating from p_r; see Figure 2.4. For r_1 small, this follows from the implicit function theorem. Actually, $S_{a,1}$ and $S_{r,1}$ are precisely the branches of the critical manifold S described in section 2.1; this also explains the notation. Along the curve $S_{a,1}$ the linearization of (2.18) has one zero eigenvalue, the other eigenvalue is negative and close to -2 for r_1 small. Along $S_{r,1}$ the situation is similar; however, the nonzero eigenvalue is positive and close to 2 for r_1 small.

Remark 2.7. Equation (2.18) is the directional (in the positive y-direction) blow-up of the fold point $(0, 0)$ of the layer problem, i.e., system (1.2) with $\varepsilon = 0$. The line $l_1 = 0$ corresponds to the fold point. We have gained normal hyperbolicity of the lines of equilibria $S_{a,1}$ (resp., $S_{r,1}$) at the points p_a (resp., p_r) due to the blow-up (compare Figure 2.2).

The dynamics in the invariant plane $r_1 = 0$ is governed by

$$(2.19) \qquad \begin{aligned} x_1' &= -1 + x_1^2 + \frac{1}{2}\varepsilon_1 x_1, \\ \varepsilon_1' &= \frac{3}{2}\varepsilon_1^2 \,. \end{aligned}$$

We recover the equilibria points p_a and p_r; however, there exists an additional zero eigenvalue due to the second equation. The corresponding eigenvector is $(-1, 4)$ at both equilibria. Hence, there exist one-dimensional center manifolds $N_{a,1}$ at p_a and $N_{r,1}$ at p_r along which ε_1 increases for $\varepsilon_1 > 0$. Note that the branch of the attracting center manifold $N_{a,1}$ at p_a in the half space $\varepsilon_1 > 0$ is unique, while the repelling center manifold $N_{r,1}$ at p_r in the half space $\varepsilon_1 > 0$ is not unique; see Figure 2.4. We collect the information we have obtained so far in the following lemma.

LEMMA 2.5. *The linearization of system* (2.17) *at* p_j, $j = a, r$ *has the following real eigenvalues:* $\lambda_1 = -2$ *at* p_a *and* $\lambda_1 = 2$ *at* p_r *with eigenvector* $(1, 0, 0)$ *corresponding to the flow on* l_1, $\lambda_2 = 0$ *with an eigenvector tangent to* $S_{j,1}$, *and* $\lambda_3 = 0$ *with an eigenvector* $(-1, 0, 4)$ *corresponding to the center direction in the invariant plane* $r_1 = 0$.

We restrict our attention to the set

$$D_1 := \{(x_1, r_1, \varepsilon_1) : \ x_1 \in \mathbb{R}, 0 \leq r_1 \leq \rho, \ 0 \leq \varepsilon_1 \leq \delta\},$$

where $\rho > 0$ is the constant defining the sections Δ^{in} and Δ^{out} in section 2.1 and $\delta > 0$ is the constant defining the sections Σ_2^{in} and Σ_2^{out} in section 2.4. Note that all objects defined later extend smoothly to negative values of r_1 and ε_1; i.e., there are no problems due to the boundaries $r_1 = 0$ and $\varepsilon_1 = 0$. We have the following result.

PROPOSITION 2.6. *For* ρ, δ *sufficiently small the following assertions hold for system* (2.17):

1. *There exists an attracting two-dimensional* C^k-*center manifold* $M_{a,1}$ *at* p_a *which contains the line of equilibria* $S_{a,1}$ *and the center manifold* $N_{a,1}$. *In* D_1 *the manifold* $M_{a,1}$ *is given as a graph* $x_1 = h_a(r_1, \varepsilon_1)$. *The branch of* $N_{a,1}$ *in* $r_1 = 0$, $\varepsilon_1 > 0$ *is unique.*

2. *There exists a repelling two-dimensional C^k-center manifold $M_{r,1}$ at p_r which contains the line of equilibria $S_{r,1}$ and the center manifold $N_{r,1}$. In D_1 the manifold $M_{r,1}$ is given as a graph $x_1 = h_r(r_1, \varepsilon_1)$. The branch of $N_{r,1}$ in $r_1 = 0$, $\varepsilon_1 > 0$ is not unique.*

3. *There exists a stable invariant foliation $\mathcal{F}^s$ with base $M_{a,1}$ and one-dimensional fibers. For any $c > -2$ there exists a choice of positive ρ and δ such that the contraction along $\mathcal{F}^s$ during a time interval $[0, T]$ is stronger than e^{cT}.*

4. *There exists an unstable invariant foliation $\mathcal{F}^u$ with base $M_{r,1}$ and one-dimensional fibers. For any $c < 2$ there exists a choice of positive ρ and δ such that the expansion along $\mathcal{F}^u$ during a time interval $[0, T]$ is stronger than e^{cT}.*

5. *The unique branch of $N_{a,1}$ in $r_1 = 0$, $\varepsilon_1 > 0$ is equal to $\gamma_1 := \kappa_{12}^{-1}(\gamma_2)$, wherever κ_{12}^{-1} is defined, i.e., along the part of γ_2 corresponding to $y_2 > 0$.*

Proof. Assertions (1)–(4) follow from Lemma 2.5 and center manifold theory; see, e.g., [4], [10]. Proposition 2.3 and the coordinate transformation (2.12) imply that $\kappa_{12}^{-1}(\gamma_2)$ has the expansion

$$\left(x_2 \left(x_2^2 + \frac{1}{2x_2} + O\left(\frac{1}{x_2^4}\right) \right)^{-1/2}, \; 0, \; \left(x_2^2 + \frac{1}{2x_2} + O\left(\frac{1}{x_2^4}\right) \right)^{-3/2} \right)$$

as $x_2 \to -\infty$. Expanding these terms in powers of x_2 shows that $\kappa_{12}^{-1}(\gamma_2)$ converges to p_a tangent to the center-direction $(-1, 0, 4)$ as $x_2 \to -\infty$. This and the uniqueness of the branch of $N_{a,1}$ in $r_1 = 0$, $\varepsilon_1 > 0$ imply assertion (5).   □

Remark 2.8. Clearly, the center manifold $M_{a,1}$ in chart K_1 corresponds to a locally invariant manifold $\bar{M}_a$ of the blown-up vector field $\bar{X}$. The importance of assertion (5) in the above proposition is that it allows us to track the manifold $\bar{M}_a$ as it moves across the sphere S^2 guided by the special orbit $\bar{\gamma}$ corresponding to the solution γ_2 of the Riccati equation.

We now define the following sections:

$$\Sigma_1^{in} := \{(x_1, r_1, \varepsilon_1) \in D_1 \; : \; r_1 = \rho\}, \quad \Sigma_1^{out} := \{(x_1, r_1, \varepsilon_1) \in D_1 \; : \; \varepsilon_1 = \delta\}.$$

Remark 2.9. Note that Σ_1^{in} maps under the blow-up transformation (2.8) to Δ^{in} and Σ_1^{out} maps under the coordinate transformation (2.11) to Σ_2^{in}. An important part of our description of the flow near the fold is the description of the transition map from Σ_1^{in} to Σ_1^{out} near the center manifolds $M_{a,1}$ and $M_{r,1}$. Since the neighborhood of $M_{a,1}$ corresponds to the neighborhood of the attracting branch of the slow manifold of (1.2), we are more interested in understanding the dynamics near $M_{a,1}$. Yet the analysis of the two cases is very similar, so we handle them simultaneously.

Let R_1 be the rectangle in Σ_1^{in} defined by $|1+x_1| \leq \beta_1$, and let R_2 be the rectangle in Σ_1^{out} defined by $|1 - x_1| \leq \beta_1$ for sufficiently small $\beta_1 > 0$. The constants ρ, δ, and β_1 can be chosen such that $M_{a,1} \cap \Sigma_1^{in} \subset R_1$ and $M_{r,1} \cap \Sigma_1^{out} \subset R_2$. For $0 \leq \tilde{\varepsilon} \leq \delta$ and $0 \leq \tilde{r} \leq \rho$, let $I_a(\tilde{\varepsilon})$ be the line $R_1 \cap \{\varepsilon_1 = \tilde{\varepsilon}\}$ and $I_r(\tilde{r})$ be the line $R_2 \cap \{r_1 = \tilde{r}\}$.

In the neighborhood of p_j, $j = a, r$, the flow of (2.17) carries Σ_1^{in} to Σ_1^{out}. Let $\Pi_1 : \Sigma_1^{in} \to \Sigma_1^{out}$ be the transition map defined by the flow of (2.17). The map Π_1 is well defined on R_1, at least for small enough values of ρ, δ, and β_1. The map Π_1 is defined in a wedge-shaped set in Σ_1^{in} around $M_{r,1}$ that shrinks to $S_{r,1}$ for $\varepsilon_1 \to 0$. The reason for this difference is that $M_{a,1}$ is attracting and $M_{r,1}$ is repelling. We have the following estimate of transition times.

LEMMA 2.7. *The transition time T of a solution of system (2.17) from a point $p = (x_1, \rho, \varepsilon_1) \in \Sigma_1^{in}$ to the point $\Pi_1(p) \in \Sigma_1^{out}$ satisfies*

$$(2.20) \qquad T = \frac{2}{3}\left(\frac{1}{\varepsilon_1} - \frac{1}{\delta}\right)(1 + O(\rho)).$$

Proof. The evolution of ε_1 determines the transition time of solutions from Σ_1^{in} to Σ_1^{out}. The relevant equation is

$$(2.21) \qquad \varepsilon_1' = \frac{3}{2}\varepsilon_1^2(1 - O(r_1)).$$

The result follows immediately by integrating (2.21).   □

PROPOSITION 2.8. *For ρ, δ, and β_1 sufficiently small the transition map Π_1 : $\Sigma_1^{in} \to \Sigma_1^{out}$ defined by the flow of system (2.17) has the following properties:*
  1. *$\Pi_1(R_1)$ is a wedge-like region in Σ_1^{out}. $\Pi_1^{-1}(R_2)$ is a wedge-like region in Σ_1^{in}.*
  2. *More precisely, for fixed $c < 2$ there exists a constant K depending on the constants c, ρ, δ, and β_1 such that*
     (i) for $\varepsilon_1 \in (0, \delta]$ the map $\Pi_1|_{I_a(\varepsilon_1)}$ is a contraction with contraction rate bounded by $Ke^{-\frac{2c}{3}\left(\frac{1}{\varepsilon_1} - \frac{1}{\delta}\right)}$.
     (ii) for $r_1 \in (0, \rho]$ the map $\Pi_1^{-1}|_{I_r(r_1)}$ is a contraction with contraction rate bounded by $Ke^{-\frac{2c}{3}\left(\frac{\rho^3}{r_1^3\delta} - \frac{1}{\delta}\right)}$.

Proof. The assertions follow from Proposition 2.6 and Lemma 2.7. The estimate for the contraction rate of Π_1^{-1} in the second assertion uses the identity $\varepsilon_1\rho^3 = \delta r_1^3$ for $p = (x_{1,in}, \rho, \varepsilon_1)$ and $\Pi_1(p) = (x_{1,out}, r_1, \delta)$ to express the transition time in terms of r_1.   □

All our results concerning the dynamics in chart K_1 are illustrated in Figure 2.4.

2.6. Dynamics in chart K_3. We use chart K_3 to analyze the dynamics of the blown-up vector field $\bar{X}$ in a neighborhood of the equator containing the point q_{out}. Applying transformation (2.10) to system (2.5) and desingularizing by dividing out the factor r_3, we obtain

$$(2.22) \qquad \begin{aligned} r_3' &= r_3 F(r_3, y_3, \varepsilon_3), \\ y_3' &= \varepsilon_3(-1 + O(r_3)) - 2y_3 F(r_3, y_3, \varepsilon_3), \\ \varepsilon_3' &= -3\varepsilon_3 F(r_3, y_3, \varepsilon_3), \end{aligned}$$

where $F(r_3, y_3, \varepsilon_3) := 1 - y_3 + O(r_3)$. The planes $\varepsilon_3 = 0$ and $r_3 = 0$ and the y_3-axis are invariant under the flow of (2.22).

LEMMA 2.9. *The point $q_{out} = (0, 0, 0)$ is a hyperbolic equilibrium of system (2.22) with eigenvalues: $\lambda_1 = 1$ with eigenvector $(1, 0, 0)$ corresponding to the flow in $\varepsilon_3 = 0$, $\lambda_2 = -2$ with eigenvector $(0, 1, 0)$ corresponding to the flow on the y_3-axis, and $\lambda_3 = -3$ with eigenvector $(0, 1, 1)$ corresponding to the flow in $r_3 = 0$.*

Proof. Computation.   □

Now we transform the part of the special orbit γ_2 (introduced in Proposition 2.3) corresponding to $x_2 > 0$ to chart K_3; i.e., we define $\gamma_3 := \kappa_{23}(\gamma_2)$.

LEMMA 2.10. *The orbit γ_3 lies in the plane $r_3 = 0$, converges to q_{out} as $\varepsilon_3 \to 0$, and is tangent at q_{out} to the vector $(0, 1, 0)$.*

Proof. The coordinate transformation (2.13) and assertion (3) from Proposition 2.3 imply that the orbit γ_3 has the expansion $(0, -\Omega_0\varepsilon_3^{2/3} + \varepsilon_3 + O(\varepsilon_3^{5/3}), \varepsilon_3)$ as $\varepsilon_3 \to 0$. The lemma follows.   □

Lemma 2.10 implies that parts of the manifold $\bar{M}_a$ corresponding to $\bar{r} > 0$ come close to the equilibrium q_{out}. Hence, we need a precise description of the dynamics of system (2.22) close to q_{out}. This is a somewhat delicate problem because of the *resonance* $\lambda_2 = \lambda_1 + \lambda_3$, which implies that there exists no smooth transformation of the nonlinear flow to the flow of the corresponding linearization. It turns out that, due to the simple form of the equations, it is quite easy to work out the lowest order approximation of the flow.

For the description of the flow in a neighborhood of q_{out} we define sections Σ_3^{in} and Σ_3^{out} as follows:

$$\Sigma_3^{in} = \{(r_3, y_3, \varepsilon_3) \ : \ r_3 \in [0, \rho], \ y_3 \in [-\beta_3, \beta_3], \ \varepsilon_3 = \delta\},$$
$$\Sigma_3^{out} = \{(r_3, y_3, \varepsilon_3) \ : \ r_3 = \rho, \ y_3 \in [-\beta_3, \beta_3], \ \varepsilon_3 \in [0, \delta]\},$$

where ρ and δ are the same constants as before, and $\beta_3 > 0$ is sufficiently small; see Figure 2.5.

Let Π_3 be the transition map from Σ_3^{in} to Σ_3^{out}. Our goal is to obtain a formula for the map Π_3. Before stating the relevant result we need to discuss the structure of (2.22) in more detail. We first divide (2.22) by the factor $F(r_3, y_3, \varepsilon_3)$, which is close to one near q_{out}, and obtain

$$(2.23) \qquad \begin{aligned} r_3' &= r_3, \\ y_3' &= -2y_3 - \frac{\varepsilon_3}{1 - y_3} + r_3 \varepsilon_3 G(r_3, y_3, \varepsilon_3), \\ \varepsilon_3' &= -3\varepsilon_3, \end{aligned}$$

where $G(r_3, y_3, \varepsilon_3)$ is a C^k-function. Consider (2.23) with $r_3 = 0$, namely,

$$(2.24) \qquad \begin{aligned} y_3' &= -2y_3 - \frac{\varepsilon_3}{1 - y_3}, \\ \varepsilon_3' &= -3\varepsilon_3. \end{aligned}$$

By construction, system (2.24) is, up to rescaling of time, the Riccati equation (2.16) transformed to K_3. The corresponding linearization has eigenvalues $\lambda_2 = -2$ and $\lambda_3 = -3$; hence, (2.16) can be linearized by a near identity transformation of the form

$$(2.25) \qquad y_3 = \psi(\tilde{y}_3, \varepsilon_3),$$

where the function ψ is C^k smooth and $\psi(\tilde{y}_3, \varepsilon_3) = \tilde{y}_3 + O(\tilde{y}_3 \varepsilon_3)$; see [22]. The corresponding inverse transformation is denoted by $\tilde{y}_3 = \tilde{\psi}(y_3, \varepsilon_3) = y_3 + O(y_3 \varepsilon_3)$. Under the transformation (2.25) system (2.23) becomes

$$(2.26a) \qquad r_3' = r_3,$$
$$(2.26b) \qquad \tilde{y}_3' = -2\tilde{y}_3 - \varepsilon_3 + r_3 \varepsilon_3 H(r_3, \tilde{y}_3, \varepsilon_3),$$
$$(2.26c) \qquad \varepsilon_3' = -3\varepsilon_3,$$

with a C^k-function H. We have the following result.

PROPOSITION 2.11. *The transition map* Π_3 *for system* (2.22) *has the form*

$$\Pi_3(r_3, y_3, \delta) = \begin{pmatrix} \rho \\ \Pi_{32}(r_3, y_3, \delta) \\ \left(\frac{r_3}{\rho}\right)^3 \delta \end{pmatrix}$$

with $\Pi_{32}(r_3, y_3, \delta)$ *given by*

$$\Pi_{32}(r_3, y_3, \delta) = (\tilde{\psi}(y_3, \delta) - \delta)\left(\frac{r_3}{\rho}\right)^2 + O(r_3^3 \ln r_3).$$

Proof. In the following we suppress the subscript 3 in system (2.26). Fix $(r_i, \tilde{y}_i, \delta) \in \Sigma^{in}$ and $(\rho, \tilde{y}_o, \varepsilon_o) \in \Sigma^{out}$. Consider a solution $(r, \tilde{y}, \varepsilon)(t)$ of (2.26) and $T > 0$ such that $r(0) = r_i$, $r(T) = \rho$, $\tilde{y}(0) = \tilde{y}_i$, $\tilde{y}(T) = \tilde{y}_o$, $\varepsilon(0) = \delta$, $\varepsilon(T) = \varepsilon_o$. We will now compute $(T, \tilde{y}_o, \varepsilon_o)$ as a function of $(r_i, \tilde{y}_i)$. Equations (2.26a) and (2.26c) have explicit solutions $r = e^t r_i$, $\varepsilon = \delta e^{-3t}$. The requirement $r(T) = \rho$ produces an expression for T, namely,

$$(2.27) \qquad T = \ln\left(\frac{\rho}{r_i}\right).$$

Let z be a new coordinate defined by $\tilde{y} = e^{-2t}(\tilde{y}_i - \delta + z) + \delta e^{-3t}$. We get the following equation for z:

$$(2.28) \qquad z' = r_i H^z(z, r_i, \tilde{y}_i, t),$$

where $H^z(z, r_i, \tilde{y}_i, t) = \delta H(e^t r_i, e^{-2t}(\tilde{y}_i - \delta + z) + \delta e^{-3t}, \delta e^{-3t})$. The transition time T is still given by (2.27). Note that the function H^z is uniformly bounded on the relevant domain. Using (2.28) we obtain $z(T) = r_i O(T) = O(r_i \ln(\frac{\rho}{r_i}))$. It follows that

$$(2.29) \qquad \tilde{y}(T) = (\tilde{y}_i - \delta)\left(\frac{r_i}{\rho}\right)^2 + O\left(\frac{r_i^3}{\rho^2}\ln\left(\frac{\rho}{r_i}\right)\right).$$

Hence

$$\Pi_{32}(r_3, y_3, \delta) = \psi\left((\tilde{\psi}(y_3, \delta) - \delta)\left(\frac{r_3}{\rho}\right)^2 + O(r_3^3 \ln r_3), \left(\frac{r_3}{\rho}\right)^3 \delta\right)$$

$$= (\tilde{\psi}(y_3, \delta) - \delta)\left(\frac{r_3}{\rho}\right)^2 + O(r_3^3 \ln r_3)$$

and the result follows. $\square$

Remark 2.10. The following observation will be used later in this paper to obtain the leading order asymptotics of the extended slow manifold $S_{a,\varepsilon}$. The y_3 coordinate of the point where the special orbit γ_3 intersects the section Σ_3^{in} is $y_3^* = \delta^{2/3} s(\delta^{-1/3})$ (see the proof of Lemma 2.10). By comparing the asymptotics of γ_3 and the exact solution of system (2.26) restricted to $r_3 = 0$, i.e., the Riccati equation written in the linearizing coordinates $(\tilde{y}_3, \varepsilon_3)$, it follows that $\tilde{\psi}(y_3^*, \delta) - \delta = -\Omega_0 \delta^{2/3}$.

2.7. Phase portrait on the upper part of S^2. The sphere S^2 is invariant under the desingularization of the blown-up vector field $\bar{X}$. The equator S^1 is invariant. On S^1 there are four equilibria p_a, p_r, q_{in}, q_{out}. These equilibria are hyperbolic for the flow on S^1, the points p_a and q_{out} are attracting, and p_r and q_{in} are repelling. All orbits in $S^{2,+}$ are forward asymptotic to q_{out}. The special orbit $\bar{\gamma}$ is backward asymptotic to p_a and, as it arrives at q_{out}, it is tangent to S^1. Besides $\bar{\gamma}$ there exist two families of trajectories: backward asymptotic to p_r or backward asymptotic to q_{in}. The corresponding phase portrait of S^2 is shown in Figure 2.6.
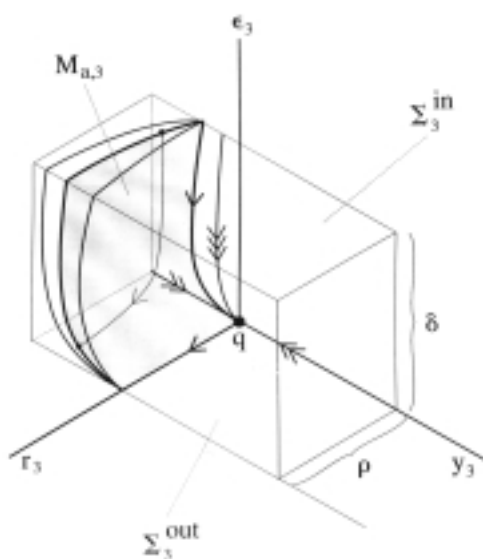
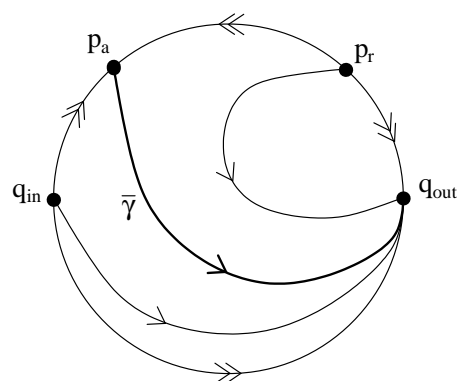FIG. 2.5. *Geometry and dynamics of system* (2.22) *near the equilibrium* q_{out}.

FIG. 2.6. *Blow-up of a fold (jump) point restricted to* S^2.

2.8. Proof of the main result. In this section we prove Theorem 2.1 by combining the results obtained in the individual charts. The idea of the proof is to analyze the evolution of the center manifold $M_{a,1}$ and the rectangle R_1 under the flow of the blown-up vector field $\bar{X}$. We denote the corresponding global invariant manifold by $\bar{M}_a$. The intersection of $\bar{M}_a$ with $S^{2,+}$ is the special orbit $\bar{\gamma}$ connecting the equilibria p_a and q_{out}. It follows that a trajectory starting in or nearby $\bar{M}_a$ will remain close to $\bar{\gamma}$ until it reaches the vicinity of q_{out}. There the trajectory follows the local dynamics near q_{out} and is repelled in the unstable direction of q_{out}.

Proof of Theorem 2.1. We define the map $\Pi : \Sigma_1^{in} \to \Sigma_3^{out}$ by

$$\Pi := \Pi_3 \circ \kappa_{23} \circ \Pi_2 \circ \kappa_{12} \circ \Pi_1.$$

The map Π is the transition map from Σ_1^{in} to Σ_3^{out} for the flow induced by the blown-up vector field $\bar{X}$ on B. We will analyze $\Pi(R_1 \cap M_{a,1})$ and then use the fact that, by construction, the transition map π is given by $\pi = \Phi \circ \Pi \circ \Phi^{-1}$ for $\varepsilon > 0$.

It follows from Proposition 2.8 that $\Pi_1(R_1 \cap M_{a,1}) \subset \Sigma_1^{out}$ is a smooth curve transverse to the set $\{r_1 = 0\}$. It follows that $\kappa_{12}(\Pi_1(R_1 \cap M_{a,1}))$ is a smooth curve transverse to the plane $\{r_2 = 0\}$. Proposition 2.4 implies that the image of this curve under Π_2 has the form $\{(\delta^{-1/3}, h_2^{out}(r_2), r_2) : r_2 \in [0, \rho\delta^{1/3}]\}$, where $h_2^{out} : [0, \rho\delta^{1/3}] \to \mathbb{R}$ is a smooth function. Under the transformation κ_{23}, this curve transforms to a smooth curve of the form $\{(r_3, h_3^{in}(r_3), \delta) : r_3 \in [0, \rho]\}$ with $(0, h_3^{in}(0), \delta) = \kappa_{23}(\gamma_2 \cap \Sigma_2^{out})$. Proposition 2.11 now implies that $\Pi(R_1 \cap M_{a,1})$ has the form $\{(\rho, h_3^{out}(\varepsilon_3), \varepsilon_3) : \varepsilon_3 \in [0, \delta]\}$, where $h_3^{out}(\varepsilon_3) = O(\varepsilon_3^{2/3})$. This proves assertion (1) of the theorem.

We now prove assertion (2). It follows from Proposition 2.8 that $\Pi_1(R_1)$ is a wedge-like region around $\Pi(R_1 \cap M_{a,1})$ of width $O(e^{-c/\varepsilon_1})$, where $c > 0$ is some constant. Since κ_{12}, Π_2 and κ_{23} are diffeomorphisms restricted to Σ_1^{out}, Σ_2^{in}, and Σ_2^{out}, respectively, it follows that $\kappa_{23} \circ \Pi_2 \circ \kappa_{12} \circ \Pi_1(R_1)$ is also a wedge-like region of width $O(e^{-c/\varepsilon_1})$ around $\kappa_{23} \circ \Pi_2 \circ \kappa_{12} \circ \Pi_1(R_1 \cap M_{a,1})$. Finally, we apply Proposition 2.11 to conclude that $\Pi(R_1)$ is a wedge-like region of width $O(e^{-c/\varepsilon_1})$ around $\Pi(R_1 \cap M_{a,1})$. The evolution of R_1 in the three charts is shown in Figure 2.7. Because $\varepsilon = \rho^3\varepsilon_1 = \rho^3\varepsilon_3$ is a constant of motion for the flow of $\bar{X}$, lines $\varepsilon_1 = \varepsilon/\rho^3$ in Σ_1^{in} are mapped to lines $\varepsilon_3 = \varepsilon/\rho^3$ in Σ_3^{out}. Restricted to such lines the map Π is a contraction with contraction rate $O(e^{-c/\varepsilon_1})$ for some $c > 0$. Assertion (2) follows by applying the appropriate blow-down transformations. $\square$

The dynamics of the blown-up vector field $\bar{X}$, and in particular the center manifold $\bar{M}_a$, are shown in Figure 2.7.

Remark 2.11. Remark 2.10 implies that the function $h_3^{out}(\varepsilon_3)$ has the asymptotic expansion

$$h_3^{out}(\varepsilon_3) = -\Omega_0\varepsilon_3^{2/3} + o(\varepsilon_3^{2/3}).$$

The corresponding expansion for the function $h(\varepsilon)$ in Theorem 2.1 is

$$h(\varepsilon) = -\Omega_0\varepsilon^{2/3} + o(\varepsilon^{2/3}).$$

This result is well known; see, e.g., [18], where it is also shown that the next term in the expansion is $O(\varepsilon \ln \varepsilon)$. Our analysis, in particular the description of the map Π_3 in Proposition 2.11, shows that the occurrence of this term is due to the resonance $\lambda_2 = \lambda_1 + \lambda_3$ at the equilibrium q_{out}; see section 2.6.
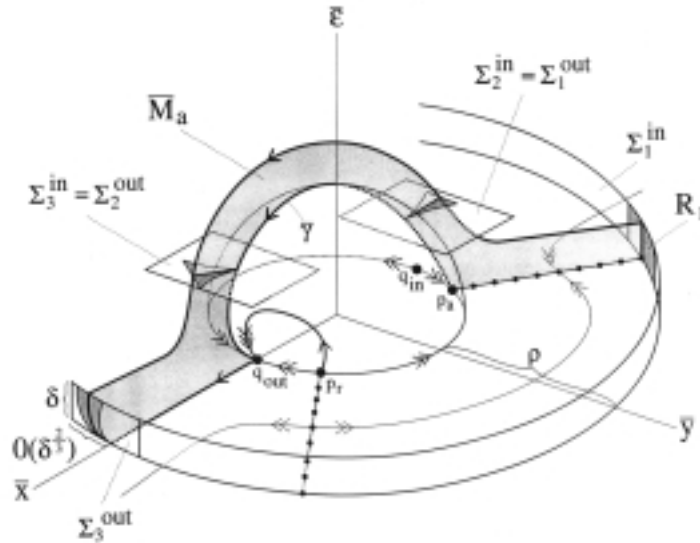
FIG. 2.7. *Geometry and dynamics of the blown-up vector field* $\bar{X}$.

3. Canard point.

3.1. Assumptions and results. In this section we consider a one parameter family of ODEs similar to (1.2), namely,

$$
\begin{aligned}
x' &= f(x, y, \lambda, \varepsilon), \\
y' &= \varepsilon g(x, y, \lambda, \varepsilon).
\end{aligned}
$$
(3.1)

We assume that $(x_0, y_0) = (0, 0)$ is a nondegenerate fold point of the critical manifold $f(x, y, \lambda, 0) = 0$ for $\lambda_0 = 0$. We assume further that $g(0, 0, 0, 0) = 0$. This gives the following set of defining conditions for the considered singularity:

$$
f(0,0,0,0) = 0, \quad \frac{\partial f}{\partial x}(0,0,0,0) = 0, \quad g(0,0,0,0) = 0
$$
(3.2)

with the nondegeneracy assumptions

$$
\frac{\partial^2 f}{\partial x^2}(0,0,0,0) \neq 0, \quad \frac{\partial f}{\partial y}(0,0,0,0) \neq 0.
$$
(3.3)

This implies that the critical manifold has a nondegenerate fold point for λ in a suitable interval. Without loss of generality we assume that the fold point is $(0, 0)$ for all values of λ. This can always be achieved by a λ-dependent translation. The remaining nondegeneracy assumptions defining a canard point are

$$
\frac{\partial g}{\partial x}(0,0,0,0) \neq 0, \quad \frac{\partial g}{\partial \lambda}(0,0,0,0) \neq 0 \ .
$$
(3.4)

These conditions insure that the nullcline $g(x, y, \lambda, 0) = 0$ is transverse to the critical manifold S and the intersection point of S and $g(x, y, \lambda, 0) = 0$ passes through the fold point $(0, 0)$ with nonzero speed as λ varies.

Let the critical manifold S, its left and right branches S_a and S_r, and the neighborhoods U and V be defined as in section 2. The manifolds $S_{a,\varepsilon}$ and $S_{r,\varepsilon}$ exist outside of V just as they did for a simple fold. Here we ask basically the same question, namely, How can S_a and S_r be extended? The situation is, however, quite different, since, for special choices of λ and ε, $S_{a,\varepsilon}$ extends to $S_{r,\varepsilon}$. This is caused by the special structure of the slow flow for $\lambda = 0$.

As in the case of the fold point, the reduced dynamics is governed by the equation

$$(3.5) \qquad \dot{x} = \frac{g(x, \varphi(x), 0, 0)}{\varphi'(x)},$$

where $\varphi(x)$ is obtained by solving the equation $f(x, y, 0, 0)$ for y as a function of x. It follows from the above assumptions that the right-hand side of (3.5) is a smooth function at the origin. Let $x_0(t)$ denote a maximal solution of (3.5) with the property that $x_0(0) = 0$. It follows that $x_0(t)$ exists and passes through the fold point (see Figure 3.1a). If $x_0(t)$ connects S_a to S_r then, heuristically, one can expect a connection from $S_{a,\varepsilon}$ to $S_{r,\varepsilon}$. In what follows we show that such a connection exists along a curve in the (λ, ε)-plane.

Remark 3.1. The case when $x_0(t)$ connects S_r to S_a can also be treated with the methods of this article, but it is less interesting and will be omitted.
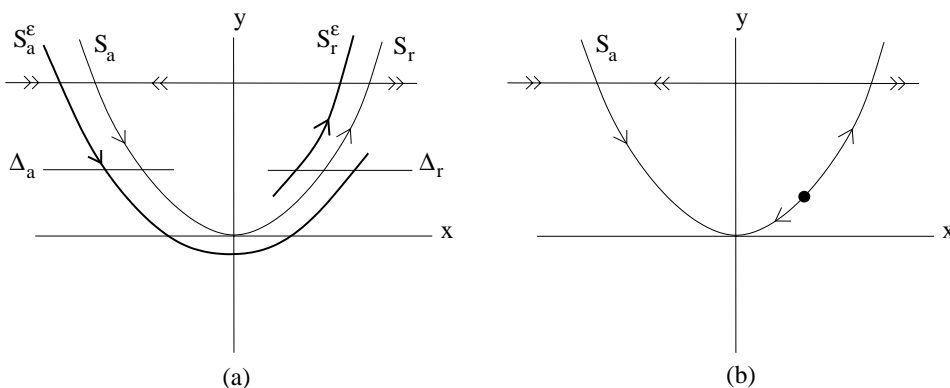

FIG. 3.1. *Reduced flow.* (a) $\lambda = 0$, (b) $\lambda > 0$.

It follows from assumptions (3.2) and (3.3) that using simple coordinate changes (scaling and translations) one can transform (3.1) to the canonical form

$$x' = -yh_1(x, y, \lambda, \varepsilon) + x^2 h_2(x, y, \lambda, \varepsilon) + \varepsilon h_3(x, y, \lambda, \varepsilon),$$
$$(3.6) \qquad y' = \varepsilon \left(\pm x h_4(x, y, \lambda, \varepsilon) - \lambda h_5(x, y, \lambda, \varepsilon) + y h_6(x, y, \lambda, \varepsilon) \right),$$

where

$$h_3(x, y, \lambda, \varepsilon) = O(x, y, \lambda, \varepsilon),$$
$$h_j(x, y, \lambda, \varepsilon) = 1 + O(x, y, \lambda, \varepsilon), \quad j = 1, 2, 4, 5.$$

We assume that the sign in front of the term xh_4 is positive. In this case, $x_0(t)$ connects S_a to S_r. Clearly, the signs of the various terms in the above equation

correspond to a certain choice of signs in the nondegeneracy conditions made earlier. The parameter λ has been rescaled such that the reduced flow has an equilibrium on S_r for $\lambda > 0$ (see Figure 3.1b).

We introduce the following notation:

$$a_1 = \frac{\partial h_3}{\partial x}(0,0,0,0), \quad a_2 = \frac{\partial h_1}{\partial x}(0,0,0,0), \quad a_3 = \frac{\partial h_2}{\partial x}(0,0,0,0),$$

$$a_4 = \frac{\partial h_4}{\partial x}(0,0,0,0), \quad a_5 = h_6(0,0,0,0),$$

and define

$$(3.7) \qquad\qquad A = -a_2 + 3a_3 - 2a_4 - 2a_5.$$

The constant A will show up in various computations and results related to the analysis of the dynamics near the canard point. In particular, we will need the genericity condition $A \neq 0$ in the analysis of canard explosion in [14].

For $j = a, r$ let $\Delta_j = \{(x, \rho^2), x \in I_j\}$ be a section of S_j near the fold point with ρ sufficiently small and suitable intervals I_j (see Figure 3.1a). Define $q_{j,\varepsilon} = \Delta_j \cap S_{j,\varepsilon}$. Let π be the transition map for the flow of (3.1) from Δ_a to Δ_r. The following theorem describes the behavior of $S_{a,\varepsilon}$ and $S_{r,\varepsilon}$ near the canard point.

THEOREM 3.1. *Assume that system* (3.1) *satisfies the defining conditions* (3.2)–(3.4) *of a canard point. Assume that the solution* $x_0(t)$ *of the reduced problem connects* S_a *to* S_r. *Then there exists* $\varepsilon_0 > 0$ *and a smooth function* $\lambda_c(\sqrt{\varepsilon})$ *defined on* $[0, \varepsilon_0]$ *such that for* $\varepsilon \in (0, \varepsilon_0]$ *the following assertions hold:*

1. $\pi(q_{a,\varepsilon}) = q_{r,\varepsilon}$ *if and only if* $\lambda = \lambda_c(\sqrt{\varepsilon})$.
2. *The function* λ_c *has the expansion*

$$(3.8) \qquad \lambda_c(\sqrt{\varepsilon}) = -\left(\frac{a_1 + a_5}{2} + \frac{1}{8}A \right) \varepsilon + O(\varepsilon^{3/2}).$$

3. *The transition map* π *is defined only for* λ *in an interval around* $\lambda_c(\sqrt{\varepsilon})$ *of width* $O(e^{-c/\varepsilon})$ *for some* $c > 0$.
4.

$$\left. \frac{\partial}{\partial \lambda}(\pi(q_{a,\varepsilon}) - q_{r,\varepsilon}) \right|_{\lambda = \lambda_c(\sqrt{\varepsilon})} > 0.$$

Remark 3.2. For $\lambda = \lambda_c(\sqrt{\varepsilon})$ the slow manifold $S_{a,\varepsilon}$ extends to the slow manifold $S_{r,\varepsilon}$, i.e., the slow manifold consists of a single *canard solution*. We use the term canard solution only for solutions with this property. In other works all solutions of system (1.1) which follow $S_{r,\varepsilon}$ for a time interval of order $O(1)$ are called canard solutions. The solution described in the above theorem is then called a *maximal canard* solution.

For the special case of the van der Pol equation the above results are contained in [6]. Here we treat the general case of a canard point and identify the important parameter A. Also, besides using the same blow-up our proof of the existence of a canard solution based on extending slow manifolds combined with a Melnikov-type argument is new.

3.2. Blow-up. The analysis in this section is, in many aspects, similar to that in section 2. In particular we apply a blow-up transformation, yet the weights (powers of r) must be different than in the case of simple fold. Furthermore, the parameter λ is now included in the blow-up. The blow-up transformation Φ maps $B = S^2 \times [-\mu, \mu] \times [0, \rho]$ to $\mathbb{R}^4$ according to

$$(3.9) \qquad x = \bar{r}\bar{x}, \quad y = \bar{r}^2\bar{y}, \quad \varepsilon = \bar{r}^2\bar{\varepsilon}, \quad \lambda = \bar{r}\bar{\lambda}.$$

The constants μ and ρ are chosen small enough such that equations (3.6) are valid in $\Phi(B)$. Let $\bar{X}$ denote the corresponding blown up vector field. In section 2 we used the charts K_1, K_2, and K_3 to obtain the dynamics of $\bar{X}$. Here charts K_1 and K_2 are sufficient to describe the relevant phenomena. In chart K_1, the blow-up transformation (3.9) is

$$(3.10) \qquad x = r_1 x_1, \quad y = r_1^2, \quad \varepsilon = r_1^2 \varepsilon_1, \quad \lambda = r_1 \lambda_1,$$

where $(x_1, r_1, \varepsilon_1, \lambda_1)$ are the coordinates in $\mathbb{R}^4$. In chart K_2, the blow-up transformation (3.9) is

$$(3.11) \qquad x = r_2 x_2, \quad y = r_2^2 y_2, \quad \varepsilon = r_2^2, \quad \lambda = r_2 \lambda_2,$$

where $(x_2, y_2, r_2, \lambda_2)$ are the coordinates in $\mathbb{R}^4$. A simple computation gives the following lemma.

LEMMA 3.2. *Let κ_{12} denote the change of coordinates from K_1 to K_2. Then κ_{12} is given by*

$$(3.12) \qquad x_2 = x_1 \varepsilon_1^{-1/2}, \quad y_2 = \varepsilon_1^{-1}, \quad r_2 = r_1 \varepsilon_1^{1/2}, \quad \lambda_2 = \varepsilon_1^{-1/2}\lambda_1 \quad for\ \varepsilon_1 > 0.$$

Similarly, $\kappa_{21} = \kappa_{12}^{-1}$ is given by

$$(3.13) \qquad x_1 = x_2 y_2^{-1/2}, \quad r_1 = r_2 y_2^{1/2}, \quad \varepsilon_1 = y_2^{-1}, \quad \lambda_1 = \lambda_2 y_2^{-1/2} \qquad for\ y_2 > 0.$$

3.3. Dynamics in chart K_2—preliminary analysis. After dividing out a factor r_2 in a manner analogous to that in section 2, the transformed equations (3.6) have the form

$$(3.14) \qquad \begin{aligned} x_2' &= -y_2 + x_2^2 + r_2 G_1(x_2, y_2) + O(r_2(\lambda_2 + r_2)), \\ y_2' &= x_2 - \lambda_2 + r_2 G_2(x_2, y_2) + O(r_2(\lambda_2 + r_2)), \end{aligned}$$

where

$$G(x_2, y_2) = \begin{pmatrix} G_1(x_2, y_2) \\ G_2(x_2, y_2) \end{pmatrix} = \begin{pmatrix} a_1 x_2 - a_2 x_2 y_2 + a_3 x_2^3 \\ a_4 x_2^2 + a_5 y_2 \end{pmatrix}.$$

Remark 3.3. It turns out that for $r_2 = \lambda_2 = 0$ the system (3.14) is integrable. For this reason the $O(r_2)$ and $O(\lambda_2)$ terms are crucial for the analysis.

Setting $r_2 = \lambda_2 = 0$ in (3.14) we obtain

$$(3.15) \qquad \begin{aligned} x_2' &= -y_2 + x_2^2, \\ y_2' &= x_2. \end{aligned}$$

Equation (3.15) is integrable. More precisely, we have the following lemma.

LEMMA 3.3. *The function*

$$(3.16) \qquad H(x_2, y_2) = \frac{1}{2}e^{-2y_2}\left(y_2 - x_2^2 + \frac{1}{2}\right)$$

is a constant of motion for (3.15).

Proof. A computation gives

$$x_2' = e^{2y_2}\frac{\partial H}{\partial y_2}(x_2, y_2),$$

$$(3.17) \qquad y_2' = -e^{2y_2}\frac{\partial H}{\partial x_2}(x_2, y_2).$$

The result follows.   □

Lemma 3.3 implies that the solutions of (3.15) are determined by the level curves of $H(x_2, y_2)$. Observe that (3.15) has an equilibrium at $(0,0)$ of center type, surrounded by a family of periodic orbits $H(x_2, y_2) = h$, $h \in (0, 1/4)$. The sets $H(x_2, y_2) = h$, $h \leq 0$, correspond to unbounded solutions. The locus of the solution determined by $h = 0$ is the parabola $x_2^2 - y_2 = 1/2$, and this solution is given by

$$\gamma_{c,2}(t_2) = (x_{c,2}(t_2), y_{c,2}(t_2)) = \left(\frac{1}{2}t_2, \frac{1}{4}t_2^2 - \frac{1}{2}\right), \quad t_2 \in \mathbb{R}.$$

The special solution $\bar{\gamma}_c$ is of central importance to the canard phenomenon. We will see that $\bar{\gamma}_c$ connects the endpoint p_a of the critical manifold S_a across the sphere S^2 to the endpoint p_r of the critical manifold S_r. As in the analysis of the fold point, the points p_a and p_r lie on the equator of S^2 and will be studied in chart K_1. Our goal is to investigate how this connection breaks under perturbation. The tool for this investigation will be a variant of the Melnikov method in which again both charts K_1 and K_2 will be used.

3.4. Dynamics in chart K_1. We proceed in a manner analogous to that in section 2.5 and obtain the following system of equations:

$$x_1' = -1 + x_1^2 + r_1(a_1\varepsilon_1 x_1 - a_2 x_1 + a_3 x_1^3) - \frac{1}{2}\varepsilon_1 x_1 F(x_1, r_1, \varepsilon_1, \lambda_1)$$

$$(3.18a) \qquad + O(r_1(r_1 + \lambda_1)),$$

$$(3.18b) \quad r_1' = \frac{1}{2}r_1\varepsilon_1 F(x_1, r_1, \varepsilon_1, \lambda_1),$$

$$(3.18c) \quad \varepsilon_1' = -\varepsilon_1^2 F(x_1, r_1, \varepsilon_1, \lambda_1),$$

$$(3.18d) \quad \lambda_1' = -\frac{1}{2}\lambda_1\varepsilon_1 F(x_1, r_1, \varepsilon_1, \lambda_1),$$

where

$$F(x_1, r_1, \varepsilon_1, \lambda_1) = x_1 - \lambda_1 + r_1(a_4 x_1^2 + a_5) + O(r_1(r_1 + \lambda_1)).$$

It suffices to consider $\lambda_1 \in (-\mu, \mu)$, where $\mu > 0$ can be chosen small. Many features of the dynamics in chart K_1 are analogous to section 2.5; therefore, we provide fewer details. The hyperplanes $r_1 = 0$, $\varepsilon_1 = 0$, and $\lambda_1 = 0$ are invariant, and the invariant line $l_1 := \{(x_1, 0, 0, 0) \ : \ x_1 \in \mathbb{R}\}$ contains two equilibria $p_a = (-1, 0, 0, 0)$ and $p_r = (1, 0, 0, 0)$ which are endpoints of lines of equilibria $S_{a,1}$ and $S_{r,1}$, respectively. For the

flow on the line l_1, the equilibrium p_a is attracting and p_r is repelling. Considered as equilibria of system (3.18), both equilibria have a triple eigenvalue zero.

In the invariant plane $r_1 = \lambda_1 = 0$ system (3.18) reduces to

$$x_1' = -1 + x_1^2 - \frac{1}{2}\varepsilon_1 x_1^2,$$

(3.19)
$$\varepsilon_1' = -\varepsilon_1^2 x_1.$$

Consequently, the sign of ε_1' is negative for initial conditions near p_r, which implies that the repelling center manifold $N_{r,1}$ at p_r in the half space $\varepsilon_1 > 0$ is unique. The attracting center manifold $N_{a,1}$ at p_a in the half space $\varepsilon_1 > 0$ is also unique, just as in section 2.5. Let

$$D_1 := \{(x_1, r_1, \varepsilon_1, \lambda_1) : -2 < x_1 < 2, 0 \le r_1 \le \rho, 0 \le \varepsilon_1 \le \delta, -\mu < \lambda_1 < \mu\},$$

where δ, ρ, and μ will be chosen small.

PROPOSITION 3.4. *Choose* $c_1 < 2 < c_2$. *The constants* ρ, δ *and* μ *can be chosen sufficiently small such that the following assertions hold for system* (3.18):

1. *There exists an attracting three-dimensional C^k-center manifold $M_{a,1}$ at p_a that contains the line of equilibria $S_{a,1}$ and the center manifold $N_{a,1}$. In D_1 the manifold $M_{a,1}$ is given as a graph $x_1 = h_a(r_1, \varepsilon_1, \lambda_1)$. The branch of $N_{a,1}$ in $r_1 = \lambda_1 = 0$, $\varepsilon_1 > 0$ is unique and equal to $\gamma_{c,1} := \kappa_{21}(\gamma_{c,2})$, where $\gamma_{c,2}$ is the part of the special trajectory introduced in section 3.3, corresponding to x_2 close to $-\infty$.*
2. *There exists a repelling three-dimensional C^k-center manifold $M_{r,1}$ at p_r which contains the line of equilibria $S_{r,1}$ and the center manifold $N_{r,1}$. In D_1 the manifold $M_{r,1}$ is given as a graph $x_1 = h_r(r_1, \varepsilon_1, \lambda_1)$. The branch of $N_{r,1}$ in $r_1 = \lambda_1 = 0$, $\varepsilon_1 > 0$ is unique and equal to $\kappa_{21}(\gamma_{c,2})$ for x_2 close to ∞.*
3. *There exists a stable invariant foliation $\mathcal{F}^s$ with base $M_{a,1}$ and one-dimensional fibers. There exist positive constants $K_{a,1}$ and $K_{a,2}$ such that the contraction along $\mathcal{F}^s$ in a time interval of length T can be estimated by $K_{a,2}e^{-c_2 T}$ from below and by $K_{a,1}e^{-c_1 T}$ from above.*
4. *There exists an unstable invariant foliation $\mathcal{F}^u$ with base $M_{r,1}$ and one-dimensional fibers. There exist positive constants $K_{r,1}$ and $K_{r,2}$ such that the expansion along $\mathcal{F}^u$ in a time interval of length T can be estimated by $K_{r,1}e^{c_1 T}$ from below and by $K_{r,2}e^{c_2 T}$ from above.*

Proof. The proof is analogous to the proof of Proposition 3.4. ☐

We now define the following sections:

$$\Sigma_{a,1}^{in} := \{(x_1, r_1, \varepsilon_1, \lambda_1) \in D_1 : r_1 = \rho, |1 + x_1| < \beta\},$$
$$\Sigma_{a,1}^{out} := \{(x_1, r_1, \varepsilon_1, \lambda_1) \in D_1 : \varepsilon_1 = \delta, |1 + x_1| < \beta\},$$
$$\Sigma_{r,1}^{in} := \{(x_1, r_1, \varepsilon_1, \lambda_1) \in D_1 : \varepsilon_1 = \delta, |1 - x_1| < \beta\},$$
$$\Sigma_{r,1}^{out} := \{(x_1, r_1, \varepsilon_1, \lambda_1) \in D_1 : r_1 = \rho, |1 - x_1| < \beta\},$$

where $\beta > 0$ is chosen small. For $j = a, r$, let $\Pi_{j,1}$ be the transition map defined by the flow of (3.18a) from section $\Sigma_{j,1}^{in}$ to $\Sigma_{j,1}^{out}$. With these definitions, results analogous to Lemma 2.7 and Proposition 2.8 hold for the canard point as well.

3.5. Phase portrait on $S_0^{2,+}$. Based on the analysis in charts K_1 and K_2, we can now describe the dynamics of $\bar{X}$ restricted to $S_0^{2,+}$, i.e., for $\bar{r} = \bar{\lambda} = 0$. The equator S^1 is invariant. On S^1 there are four equilibria: p_a, p_r, q_{in}, q_{out}. These equilibria are hyperbolic for the flow on S^1, the points p_a and q_{out} are attracting, and p_r and q_{in} are repelling. The special trajectory $\bar{\gamma}_c$ is a connecting orbit between p_a and p_r. Besides $\bar{\gamma}_c$, there are three types of orbits in $S^{2,+}$: a concentric family of periodic orbits, an equilibrium of center type, and a family of orbits joining q_{in} to q_{out}. The corresponding phase portrait is shown in Figure 3.2.
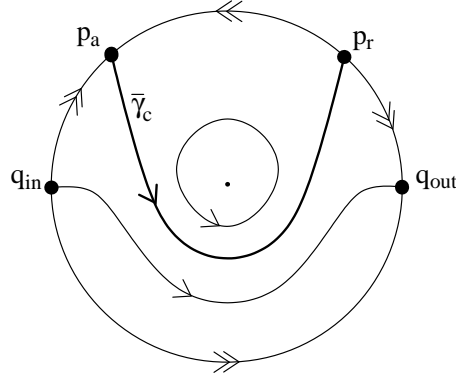

FIG. 3.2. *Blow-up of a canard point restricted to $S_0^{2,+}$ for $\bar{\lambda} = 0$.*

Remark 3.4. It turns out that the connection $\bar{\gamma}_c$ from p_a to p_r breaks for $\bar{\lambda} \neq 0$. Some important aspects of the dynamics near $S_0^{2,+}$ leading to Theorem 3.1 can be understood by investigating whether the intersection of the three-dimensional center manifolds $\bar{M}_a$ and $\bar{M}_r$ at $\bar{\gamma}_c$ is transverse. The relevant computation is carried out in the next section. Bifurcations from the center equilibrium and the family of periodic orbits and their relevance to canard explosion are studied in [14].

3.6. Melnikov computation of the separation between $M_{a,2}$ and $M_{r,2}$. The analysis of the previous sections implies that $M_{a,2}$ and $M_{r,2}$ intersect along $\gamma_{c,2}$ for $r_2 = \lambda_2 = 0$. To prove Theorem 3.1 we compute the first order separation between $M_{a,2}$ and $M_{r,2}$ with respect to r_2 and λ_2. The splitting of the manifolds off the sphere for $\lambda_2 = 0$ is shown in Figure 3.3. All functions defined below are considered as functions of $r_2 \in [0,\rho]$ and $\lambda_2 \in (-\mu,\mu)$, for small $\rho > 0$ and $\mu > 0$, without indicating this dependence explicitly. In the formulas below we drop the subscript of the time variable t_2 from chart K_2, i.e., $t = t_2$.

Let $\gamma_{a,1}$ be the trajectory of system (3.18) contained in $M_{a,1}$ for which $r_1\sqrt{\varepsilon_1} = r_2$. Let $\gamma_{a,2}(t) = (x_{a,2}(t), y_{a,2}(t))$ be the continuation of $\gamma_{a,1}$ to chart K_2, i.e., $\gamma_{a,2}$ is a solution of (3.14), parametrized such that $x_{a,2}(0) = 0$. Analogously, let $\gamma_{r,1}$ be the trajectory of (3.18) contained in $M_{r,1}$ for which $r_1\sqrt{\varepsilon_1} = r_2$ and let $\gamma_{r,2}(t) = (x_{r,2}(t), y_{r,2}(t))$ be the corresponding, backward continued solution of (3.14) parametrized such that $x_{r,2}(0) = 0$.

With these definitions, measuring the separation of $M_{a,2}$ and $M_{r,2}$ corresponds to measuring $y_{a,2}(0) - y_{r,2}(0)$, which is equivalent to estimating the *distance function*

$$(3.20) \qquad \mathcal{D}_c(r_2, \lambda_2) := H(0, y_{a,2}(0)) - H(0, y_{r,2}(0)),$$
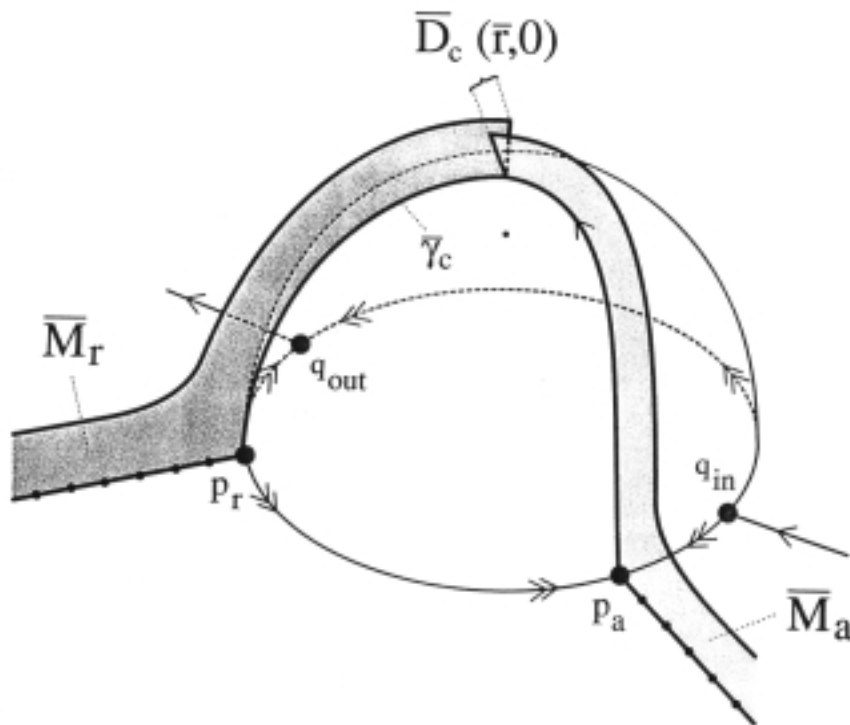
FIG. 3.3. *Splitting of $\bar{M}_a$ and $\bar{M}_r$ for $\bar{\lambda} = 0$.*

since $\frac{\partial H}{\partial y_2}(0, y_2) \neq 0$ for $y_2 < 0$. We define

$$(3.21) \qquad d_{r_2} = \int_{-\infty}^{\infty} \mathrm{grad} H(\gamma_{c,2}(t)) \cdot G(\gamma_{c,2}(t)) dt,$$

where G is the function defined in section 3.3. Similarly we define

$$(3.22) \qquad d_{\lambda_2} = \int_{-\infty}^{\infty} \mathrm{grad} H(\gamma_{c,2}(t)) \cdot \begin{pmatrix} 0 \\ -1 \end{pmatrix} dt.$$

We will prove the following result.

PROPOSITION 3.5. *For ρ and μ small enough, the distance function $\mathcal{D}_c(r_2, \lambda_2)$ is a C^k-function and has the expansion*

$$(3.23) \qquad \mathcal{D}_c(r_2, \lambda_2) = d_{r_2} r_2 + d_{\lambda_2} \lambda_2 + O(2).$$

Proof. By construction $\mathcal{D}_c$ is C^k smooth and $\mathcal{D}_c(0, 0) = 0$. Thus we have to verify the expansion. We carry out the computation for r_2. The result for λ_2 can be obtained in a similar way. We set $\lambda_2 = 0$ and consider $r_2 \in [0, \rho]$. We will show that

$$(3.24) \qquad H(0, y_{a,2}(0)) = r_2 \int_{-\infty}^{0} \mathrm{grad} H(\gamma_{c,2}(t)) \cdot G(\gamma_{c,2}(t)) dt + O(r_2^2).$$

An analogous argument yields

$$(3.25) \qquad H(0, y_{r,2}(0)) = -r_2 \int_{0}^{\infty} \mathrm{grad} H(\gamma_{c,2}(t)) \cdot G(\gamma_{c,2}(t)) dt + O(r_2^2),$$

which implies the proposition.

We define $T(r_2, \delta) < 0$ such that $y_{a,2}(T) = \delta^{-1}$, where δ is the constant from the definition of $\Sigma_{1,a}^{out}$. We write

$$H(0, y_{a,2}(0)) = H(x_{a,2}(T), \delta^{-1}) + \int_T^0 \frac{dH}{dt}(\gamma_{a,2}(t))dt.$$

By standard methods [4]

$$\int_T^0 \frac{dH}{dt}(\gamma_{a,2}(t))dt = r_2 \int_T^0 \mathrm{grad}H(\gamma_{a,2}(t)) \cdot G(\gamma_{a,2}(t))dt + O(r_2^2).$$

It turns out to be very natural to compute $H(x_{a,2}(T), \delta^{-1})$ in chart K_1. We begin by parametrizing $\gamma_{a,1}$ by ε_1, i.e.,

$$\gamma_{a,1}(\varepsilon_1) = \left(x_{a,1}(\varepsilon_1), \frac{r_2}{\sqrt{\varepsilon_1}}, \varepsilon_1, 0 \right), \quad \varepsilon_1 \in \left[\left(\frac{r_2}{\rho}\right)^2, \delta \right],$$

where ρ is the constant used in the definition of $\Sigma_{a,1}^{in}$. Let $H_1 = H \circ \kappa_{12}$, i.e.,

$$(3.26) \qquad H_1(x_1, \varepsilon_1) = H\left(\frac{x_1}{\sqrt{\varepsilon_1}}, \frac{1}{\varepsilon_1} \right) = e^{-2/\varepsilon_1} \left(\frac{1}{4} + \frac{1}{2\varepsilon_1} - \frac{x_1^2}{2\varepsilon_1} \right).$$

We wish to estimate $H_1(x_{a,1}(\delta), \delta)$. Note that $H_1(x_{a,1}((\frac{r_2}{\rho})^2), (\frac{r_2}{\rho})^2)$ is exponentially small in r_2. Hence,

$$H_1(x_{a,1}(\delta), \delta) = \int_{(\frac{r_2}{\rho})^2}^\delta \frac{d}{d\varepsilon_1} H_1(x_{a,1}(\varepsilon_1), \varepsilon_1)d\varepsilon_1 + O(r_2^2).$$

From (3.26) we obtain

$$(3.27) \qquad \begin{aligned} \frac{\partial H_1}{\partial x_1} &= -e^{-2/\varepsilon_1} \frac{x_1}{\varepsilon_1}, \\ \frac{\partial H_1}{\partial \varepsilon_1} &= e^{-2/\varepsilon_1} \frac{1}{\varepsilon_1^2} \left(\frac{1}{2}x_1^2 - \frac{x_1^2}{\varepsilon_1} + \frac{1}{\varepsilon_1} \right). \end{aligned}$$

Note that $\frac{dH_1}{d\varepsilon_1}$ evaluated along a trajectory of (3.18) is given by

$$\frac{dH_1}{d\varepsilon_1} = \frac{\partial H_1}{\partial x_1} \frac{x_1'}{\varepsilon_1'} + \frac{\partial H_1}{\partial \varepsilon_1},$$

where x_1' and ε_1' are given by (3.18a) and (3.18c), respectively. By using (3.27), expanding and using the relation $r_1 = r_2/\sqrt{\varepsilon_1}$ to eliminate r_1, we obtain the following formula for $\frac{dH_1}{d\varepsilon_1}$ evaluated along a trajectory of (3.18):

(3.28)
$$\frac{dH_1}{d\varepsilon_1}(x_1, \varepsilon_1) = e^{-2/\varepsilon_1} \varepsilon_1^{-7/2} \left[r_2(a_1 x_1 \varepsilon_1 - a_2 x_1 + a_3 x_1^3 + \frac{1-x_1^2}{x_1}(a_4 x_1^2 + a_5)) + \frac{1}{\sqrt{\varepsilon_1}} O(r_2^2) \right].$$

We set

$$(3.29) \qquad \eta(x_1, \varepsilon_1) = e^{-2/\varepsilon_1} \varepsilon_1^{-7/2} \left(a_1 x_1 \varepsilon_1 - a_2 x_1 + a_3 x_1^3 + \frac{1-x_1^2}{x_1}(a_4 x_1^2 + a_5) \right).$$

It follows that

$$\int_{(\frac{r_2}{\rho})^2}^{\delta} \frac{d}{d\varepsilon_1} H_1(x_{a,1}(\varepsilon_1), \varepsilon_1) d\varepsilon_1 = r_2 \int_{(\frac{r_2}{\rho})^2}^{\delta} \eta(x_{a,1}(\varepsilon_1), \varepsilon_1) d\varepsilon_1 + O(r_2^2),$$

where we have used that the integral of the error term in (3.28) is $O(r_2^2)$ because of the exponentially small prefactor. To complete the computation, recall that $(x_{c,1}(\varepsilon_1), \varepsilon_1)$ parametrizes $N_{a,1}$, and, by center manifold theory,

$$|x_{c,1}(\varepsilon_1) - x_{a,1}(\varepsilon_1)| = O(r_1) = O\left(\frac{r_2}{\sqrt{\varepsilon_1}}\right).$$

By using this estimate it follows that

$$H_1(x_{a,1}(\delta), \delta) = r_2 \int_0^{\delta} \eta(x_{c,1}(\varepsilon_1), \varepsilon_1) d\varepsilon_1 + O(r_2^2),$$

where we have again used the exponentially small prefactor of the integrand to estimate the error caused by first replacing $x_{a,1}$ by $x_{c,1}$ and then changing the interval of integration to $[0, \delta]$. By applying the change of variables formula, we transform this integral to chart K_2 and obtain

$$\int_0^{\delta} \eta(x_{c,1}(\varepsilon_1), \varepsilon_1) d\varepsilon_1 = \int_{-\infty}^{T} \text{grad} H(\gamma_{c,2}(t)) \cdot G(\gamma_{c,2}(t)) dt.$$

The result follows.   □

Remark 3.5. The formulas for the constants d_{r_2} and d_{λ_2} are the usual Melnikov integrals for the splitting of saddle-saddle connections for perturbations of planar Hamiltonian vector fields. However, the situation considered above is not covered by the usual Melnikov theory.

Proof of Theorem 3.1. It follows from the above results that for $(r_2, \lambda_2) \in [0, \rho) \times (-\mu, \mu)$ a connection from $S_{a,\varepsilon}$ to $S_{r,\varepsilon}$ exists if and only if

$$(3.30) \qquad \mathcal{D}_c(r_2, \lambda_2) = 0.$$

We have shown that $\mathcal{D}_c(r_2, \lambda_2) = d_{r_2} r_2 + d_{\lambda_2} \lambda_2 + O(2)$. Hence, (3.30) can be solved for λ_2 by the implicit function theorem provided that $d_{\lambda_2} \neq 0$. The solution has the expansion

$$(3.31) \qquad \lambda_2 = -\frac{d_{r_2}}{d_{\lambda_2}} r_2 + O(r_2^2).$$

By using the parametrization of $\gamma_{c,2}$ and repeated integration by parts, we compute

$$d_{r_2} = \int_{-\infty}^{\infty} e^{-2y_2}(-a_1 x_2^2 + (a_2 - a_4 + a_5)x_2^2 y_2 + (a_4 - a_3)x_2^4 - a_5 y_2^2) dt$$

$$(3.32) \qquad = -\frac{e}{4}\left(a_1 + a_5 + \frac{1}{4}A\right) \int_{-\infty}^{\infty} e^{-t^2/2} dt$$

and

$$(3.33) \qquad d_{\lambda_2} = -\int_{-\infty}^{\infty} \frac{1}{2} e^{-2y_2} dt = -\frac{e}{2} \int_{-\infty}^{\infty} e^{-t^2/2} dt.$$

This proves assertion (1). Property (2) follows by applying transformation (3.11) to the the expansion (3.31). Assertion (3) follows from the above combined with Proposition 3.4 because $M_{a,2}$ must be exponentially close to $M_{r,2}$ to reach the section $\Sigma_{r,1}^{out}$. Finally, the inequality $d_{\lambda_2} < 0$ implies that the intersection of the slow manifolds breaks as described in assertion (4).   □

Remark 3.6. It is known that the function λ_c from Theorem 3.1 which describes the canard curve actually has a power series in ε; see [3], [7], [19]. It is interesting to observe that this fact can be explained by a symmetry property of the blow-up transformation. The form of the blow-up transformation (3.9) implies that the transformation

$$(3.34) \qquad (\bar{x}, \bar{y}, \bar{r}, \bar{\lambda}) \mapsto (-\bar{x}, \bar{y}, -\bar{r}, -\bar{\lambda})$$

is a time-reversal symmetry of the blown-up vector field $\bar{X}$; i.e., it maps orbits to orbits. Note that for prescribed slow manifolds outside V, the canard curve is uniquely determined. Since the transformation (3.34) maps a canard curve to a canard curve, it follows that $-\lambda_{c,2}(r_2) = \lambda_{c,2}(-r_2)$ and consequently $\lambda_c(r_2) = \lambda_{c,2}(-r_2)$. From this we conclude that an asymptotic expansion of the canard curve is quadratic in r_2 and hence is a power series in ε. If the original vector field is smooth and the slow manifolds are chosen smooth, then, by a theorem of Schwartz [21], λ_c is a smooth function of ε.

The function λ_c depends on the choice of the slow manifolds. However all slow manifolds are exponentially close and the corresponding functions λ_c differ only by exponentially small terms and have the same asymptotic expansion.

REFERENCES

[1] V. I. ARNOLD, ED., *Dynamical Systems* V, *Bifurcation theory and catastrophe theory,* Encyclopaedia Math. Sci. 5, Springer-Verlag, Berlin, 1989.

[2] E. BENOIT, ED., *Dynamic Bifurcations*, Lecture Notes in Math. 1493, Springer, New York, 1991.

[3] E. BENOIT, J. L. CALLOT, F. DIENER, AND M. DIENER, *Chasse au canards*, Collect. Math., 31 (1981), pp. 37–119.

[4] S-N. CHOW, C. LI, AND D. WANG, *Normal Forms and Bifurcation of Planar Vector Fields*, Cambridge University Press, Cambridge, 1994.

[5] F. DUMORTIER, *Techniques in the theory of local bifurcations: Blow-up, normal forms, nilpotent bifurcations, singular perturbations*, in Bifurcations and Periodic Orbits of Vector Fields, D. Szlomiuk, ed., NATO Adv. Sci. Inst. Ser. C Math. Phys. Sci. 408, Kluwer, Dordrecht, the Netherlands, 1993, pp. 19–73.

[6] F. DUMORTIER AND R. ROUSSARIE, *Canard cycles and center manifolds*, Mem. Amer. Math. Soc. 577, Providence, 1996.

[7] W. ECKHAUS, *Relaxation oscillations including a standard chase on French ducks*, in Asymptotic Analysis II, Lecture Notes in Math. 985, Springer, New York, 1983, pp. 449–494.

[8] N. FENICHEL, *Geometric singular perturbation theory*, J. Differential Equations, 31 (1979), pp. 53–98.

[9] J. GRASMAN, *Asymptotic Methods for Relaxation Oscillations and Applications*, Springer, New York, 1987.

[10] J. GUCKENHEIMER AND P. HOLMES, *Nonlinear Oscillations, Dynamical Systems, and Bifurcations of Vector Fields*, Springer, New York, 1983.

[11] C. K. R. T. JONES, *Geometric singular perturbation theory*, in Dynamical Systems, Lecture Notes in Math. 1609, Springer, New York, 1995, pp. 44–120.

[12] J. Kevorkian and J. D. Cole, *Perturbation Methods in Applied Mathematics*, Springer, New York, 1981.

[13] M. Krupa and P. Szmolyan, *Geometric analysis of the singularly perturbed planar fold, Multiple time scale dynamical systems*, IMA Vol. Math. Appl., 122 (2000), pp. 89–116.

[14] M. Krupa and P. Szmolyan, *Relaxation oscillation and canard explosion*, J. Differential Equations, to appear, 2001.

[15] M. Krupa and P. Szmolyan, *Transcritical and pitchfork singularities of critical manifolds*, Nonlinearity, submitted, 2000.

[16] S.A. van Gils, M. Krupa, and P. Szmolyan, *Asymptotic expansions using blow-up*, Z. Angew. Math. Phys., submitted, 2000.

[17] A. Milik and P. Szmolyan, *Multiple time scales and canards in a chemical oscillator*, *Multiple time scale dynamical systems*, IMA Vol. Math. Appl., 122 (2000), pp. 117–140.

[18] E. F. Mishchenko and N. Kh. Rozov, *Differential Equations with Small Parameters and Relaxation Oscillations*, Plenum Press, New York, 1980.

[19] E. F. Mishchenko, Yu. S. Kolesov, A. Yu. Kolesov, and N. Kh. Rozov, *Asymptotic Methods in Singularly Perturbed Systems*, Monogr. Contemp. Math., Consultants Bureau, New York, 1994.

[20] L. S. Pontryagin, *Asymptotic behavior of solutions of systems of differential equations with a small parameter in derivatives of highest order*, Izv. Akad. Nauk. SSSR Ser. Mat., 21 (1957), pp. 605–626.

[21] G. Schwartz, *Smooth functions invariant under the action of a compact Lie group*, Topology, 14 (1975), pp. 63–68.

[22] S. Sternberg, *On the nature of local homeomorphisms of Euclidean n-space* II, Amer. J. Math., 80 (1958), pp. 623–631.

[23] M. Wechselberger, *Singularly Perturbed Folds and Canards in $\mathbb{R}^3$*, Ph.D. Thesis, TU-Wien, Wien, Austria, 1998.